International Journal of Physical Sciences

Volume 12 Number 22 30 November , 2017
ISSN 1992-1950

Academic Journals

ABOUT IJPS

The **International Journal of Physical Sciences (IJPS)** is published weekly (one volume per year) by Academic Journals.

International Journal of Physical Sciences (IJPS) is an open access journal that publishes high-quality solicited and unsolicited articles, in English, in all Physics and chemistry including artificial intelligence, neural processing, nuclear and particle physics, geophysics, physics in medicine and biology, plasma physics, semiconductor science and technology, wireless and optical communications, materials science, energy and fuels, environmental science and technology, combinatorial chemistry, natural products, molecular therapeutics, geochemistry, cement and concrete research, metallurgy, crystallography and computer-aided materials design. All articles published in IJPS are peer-reviewed.

Contact Us

Editorial Office: ijps@academicjournals.org

Help Desk: helpdesk@academicjournals.org

Website: http://www.academicjournals.org/journal/IJPS

Submit manuscript online http://ms.academicjournals.me/

Editors

Editorial Board

International Journal of Physical Sciences

Table of Contents: Volume 12 Number 22, 30 November, 2017

ARTICLES

academicJournals

Vol. 12(22), pp. 295-307, 30 November, 2017
DOI: 10.5897/IJPS2017.4676
Article Number: 5B0420366741
ISSN 1992 - 1950

http://www.academicjournals.org/IJPS

International Journal of Physical Sciences

Full Length Research Paper

Variability of quiet-time diurnal amplitude and phase of cosmic ray count rates in the mid- and high latitudes

Okiyi Ugochukwu[1], Okpala Kingsley C.[1,2*], Tsor James O.[1,2] and Egbunu Friday[3]

[1]Department of Physics and Astronomy, University of Nigeria, Nsukka, Enugu State, Nigeria.
[2]Department of Physics, Benue State University, Makurdi, Benue State, Nigeria.
[3]Department of Physics, Kogi State University, Anyigba, Kogi State, Nigeria.

Received 22 August, 2017; Accepted 22 September, 2017

Studies have been done on the variability of cosmic rays flux during solar quiet days at mid and high latitudes. By using the 5 quietest days for each month, the monthly mean diurnal variation of cosmic ray anisotropy have been derived for the period 1981 to 2007, which covers part of cycles 21, 22 and 23. These quiet days are days during which the sun is relatively magnetically quiet, leading to less anisotropic behaviour in the diurnal flux of cosmic rays measured on the earth surface. Four stations (Rome, Oulu, Inuvik and Thule) were used in this study to understand the important features of the high latitude and mid-latitude diurnal wave, and how solar and geomagnetic activity may be influencing the wave characteristics. Cosmic ray wave characteristics were obtained by discrete Fourier transform (DFT). The mean, diurnal amplitude, phase and dispersion for each month's diurnal wave were calculated and profiled. There was clear indication that the terrestrial effect on the variability of the monthly mean of Cosmic ray count rates was more associated with geomagnetic activity rather than rigidity of the cosmic rays. Correlation of the time series of these wave characteristics (that is, amplitude and phase) with solar and geomagnetic activity index showed better association with solar activity.

Key words: Cosmic rays, Fourier Transformation, solar quiet day, geomagnetic activity solar activity.

INTRODUCTION

Cosmic rays (CR) are high-energy charged particles originating majorly from the outer space. Their variability is a complex phenomenon which occurs all over the heliosphere and depends on many factors. No single solar index, however sophisticated can account for cosmic ray variations (Helen and Evangelos, 2012). Different scientists proposed empirical relations describing the long-term cosmic ray variations based on the joint use of solar and/or heliospheric indices. At first, solar indices such as sunspot number and solar flares were used; later Belov et al. (1999) proposed a multi-parametric description of long-term cosmic ray variations. The flux (count rate) of cosmic rays incident on the earth's upper atmosphere is varied by two processes;

*Corresponding author. E-mail: kingsley.okpala@unn.edu.ng.

solar wind and earth's magnetic field.

Solar wind purges out magnetized plasma generated by the sun, which decelerates incoming particles as well as excluding some of the particles with energies below about 1 GeV. The solar wind is not constant due to changes in solar activities; hence the level of variation changes with solar activity. Earth's magnetic field deflects some of the cosmic rays, giving rise to the observation that the intensity of cosmic radiation is dependent on latitude, longitude and azimuth angle. The geomagnetic field modulates the CR flux through the vertical geomagnetic cut-off rigidity (P_c) which can be adequately described by Stormer's equation (taking the field to be a dipole):

$$P_C = 1.9M\cos^4\lambda_G[GV]. \quad (1)$$

where M is the geomagnetic field dipole moment (in 7.96 Am^2), and λ_G is the geomagnetic latitude. Cosmic rays play an important role in the solar system and galactic astrophysics. Many researchers have tried to understand the variability of cosmic ray because of their possible effects on geophysical processes. Since cosmic ray (CR) count rates measured on Earth are affected by heliospheric and geomagnetic modulation in addition to atmospheric effects on the flux arriving from outside the heliosphere, the diurnal variation of cosmic rays is the result of a complex combination of the effects of the interplanetary magnetic field (IMF) and geomagnetic field in addition to latitude and altitude of the location of detection on Earth. The variability of cosmic ray flux on long term and short term basis has been studied extensively by quite a number of authors (Singer, 1952; Pomerantz and Duggal, 1971; Ananth et al., 1993; Okpala and Okeke, 2011; Bazilevskaya et al., 1995; Usoskin and Kalevi, 2001; Kudela et al., 2008; Sabbah and Kudela, 2011; Singh and Badruddin, 2015). The diurnal variation of CR can be characterized by the maximal value (amplitude) and phase (time of the maximal amplitude) in addition to the mean dispersion of the diurnal flux from the harmonic signatures. Simple harmonic analysis has been applied by many authors (Agarwal and Mishra, 2008; Kudela et al., 2008; Kane, 2009; Sabbah and Kudela, 2011; Okpala and Okeke, 2011; Singh and Badruddin, 2015) to understand the nature of diurnal variation of cosmic rays flux. Their statistical association with different possible drivers have also been investigated. Important findings on the solar modulation of cosmic rays are described next.

SOLAR MODULATION OF COSMIC RAYS

As expected, the sun is a dominant contributor to diurnal cosmic ray flux and atmospheric effects are expected to play significant role in the seasonal variation (Pomerantz and Duggal, 1971). Bazilevskaya et al. (1995) studied the relationship between the galactic cosmic ray intensity and the sunspot distribution. A satisfactory relationship was found between a solar activity index (that is, ηΦ index) and the galactic cosmic ray (GCR) intensity over more than three solar cycles. This product of the number of sunspot groups η and their mean heliolatitude Φ (that is, ηΦ index) also describe the GCR behavior rather well. The good correlation between the time dependence of the heliolatitude (Φ) and the HCS tilt during 1983 to 1988 enabled Bazilevskaya et al. (1995) to infer that these parameters are controlled by the large-scale solar magnetic field. Tiwari et al. (2011) studied the relationship of cosmic rays with solar activities. They suggested that the modulation of galactic cosmic rays should have a significant component controlled by the state of the interplanetary magnetic fields as they are transported out from the sun and hence there should be a solar cycle effect on the drift of the cosmic rays in the heliosphere. This was corroborated recently by many other studies (Chillingarian and Mailyan, 2009; Okpala et al., 2015; Kudela and Sabbah, 2016). Recently, Thomas et al. (2017) studied the diurnal variation of cosmic rays using decadal data. They observed common polarity effects in the amplitude of the diurnal variation for all neutron monitors used in their study.

Cosmic ray variability

Kudela et al. (2008) studied long term behaviour of the diurnal wave of cosmic ray anisotropy in relation with interplanetary magnetic field. Attempts to understand the cause and effects of the relationship between cosmic ray diurnal wave anisotropy and geomagnetic/interplanetary fields is still an active area of research (Sabbah and Kudela, 2011). Singh and Badruddin (2015) studied the short term oscillations (≤ 1 solar cycle rotation) of the solar wind parameters, galactic cosmic rays and geomagnetic indices during the solar minimum between cycles 22/23 and 23/24. They reported 7.1 days, 5.5 days, 4.4 days and 3.3 days oscillations in solar wind parameters (IMF, Bz and Ey) and geomagnetic disturbance proxies (Dst and AE) during relatively quiet periods. These quasi periodicities are likely related to the period of solar wind structures bounded with the solar magnetic field polarity, IMF and solar wind characteristics were earlier reported by Sabbah (2007). The complexity of the spatial structure of the interplanetary magnetic field (IMF) and its evolution within the heliosphere, in addition to the changes in the geomagnetic field, causes variability in contribution to the quasi-periodic variations in cosmic ray. The solar activity and solar magnetic field cyclicities contribution to the quasi periodicity of signals in CR is particularly important for long term studies (Kudela and Sabbah, 2016).

The different roles of the IMF on diurnal waves of cosmic rays during disturbed and quiet conditions are not

Table 1. Details of four neutron monitor stations used in our study.

Neutron Monitor Station	Geographic Latitude (°)	Geographic Longitude (°)	Geomagnetic Latitude (°)	Geomagnetic Longitude (°)	Cutoff Rigidity (GV)	Altitude (m)
Rome	41.90	12.52	41.85	93.69	6.32	60
Oulu	65.05	25.47	61.89	116.86	0.81	0
Inuvik	68.35	226.28	70.95	272.35	0.18	21
Thule	76.61	291.20	86.43	12.91	0.00	260

well established. For instance, low energy galactic cosmic rays with energies below few tens of GeV move mostly along lines of IMF and their intensity should peak at time of best connections of solar magnetic field with geomagnetic field (Chillingarian and Mailyan, 2009). During disturbed conditions, the evolution of the IMF is well studied and cosmic ray count rates are known to undergo established transient phenomena like ground level enhancements and Forbush effects. Studying the evolution of IMF during quiet condition is of importance for a better understanding of the effect of the IMF on the diurnal flux of cosmic rays. Firoz (2008) observed narrower distribution of IMF total magnetic field and its polarity during quiet days (when compared with disturbed days). In addition, the northward component of the IMF Bz tend to dominate during quiet period. This suggests that the quiet day distribution indicates periods of less powerful interplanetary shock waves as to affect the magnetic field of the earth.

The five international quiet days are believed to be better optimized for long term and short term studies of daily variation (Kumar et al., 1998). Firoz (2008) observed differences between days with low (quiet) and high (disturbed) diurnal waves of cosmic rays; the major difference being in the distribution of phase. According to Kudela et al. (2008), the amplitude to average ratio is a useful parameter for understanding the diurnal wave contribution to cosmic ray time signal on long term scales. However not much work has been done to understand the diurnal cosmic flux association with heliospheric forcing and geomagnetic activity. The purposes of this study therefore is to investigate the features of temporal and spatial variability of mid and high latitude cosmic ray flux during quiet geomagnetic conditions and determine solar activity dependent features of the amplitude and phase of cosmic rays diurnal variation.

SOURCES OF DATA

The data used for this project was obtained from Space Physics Interactive Data Resource (SPIDR) (http://spidr.ngdc.noaa.gov/). Table 1 shows the details of four (4) cosmic ray Neutron Monitor (NM) stations used in this work. Data used in this work comprise cosmic ray count rate from four (4) Neutron Monitor stations (Rome, Oulu, Inuvik and Thule), solar and geomagnetic activity index. The sunspot number is used here as an index of solar activity. The aa index represents the geomagnetic activity level at an invariant magnetic latitude at about 50 degrees. The daily values of the aa index are obtained from an average of the 8 values (obtained from 3-hourly interval values).

Theory and method of data analysis

In this work, the five international quietest days were employed. These days are believed to experience the least geomagnetic disturbance in a month. It is assumed in this work, that using these quiet days has the advantage of eliminating transient variations of cosmic rays (Ground Level Enhancement and Forbush Decreases) from the study. The hourly means of the five (5) quietest days were used to obtain the diurnal profile for each month. Thus one-thousand, six hundred and twenty (1,620) quietest days were used to obtain the diurnal profile for 324 months (or 27 years) which were considered in this study. Equation 2 describes the intensity (I) of hourly means of the five (5) quietest days;

$$I_i = \frac{1}{5}\sum_{j=1}^{5} C_{ij} \quad (2)$$

C_i is the raw cosmic ray count rate for a particular hour I, and j = 1 to 5 refers to the 5 international quietest days.

The monthly mean count rate, diurnal amplitude, diurnal phase and dispersion of the quiet days cosmic ray count rate for the four stations were obtained from Discrete Fourier Transform (DFT) performed on the complex diurnal time series data. Cosmic ray intensity (CRI) at the time t_i can be represented by the DFT equation (Equation 3).

$$I_i = f(t) = a_0 + \sum_{n=1}^{24}\left(r_n \cos(nt) - \phi_n\right) \quad (3)$$

where a_0 is the monthly mean count rate, r_n is the diurnal amplitude and ϕ_n is the phase of CR.

In this work, the first harmonic from our Discrete Fourier Transform was considered. Equation 4 is the dispersion relation; a measure of the fit of Equation 3.

$$d = \sum_{i=1}^{n} d^2 = \sum_{i=1}^{n} [C_i - f(t_i)]^2 = \sum_{i=1}^{n} [C_i - I_i]^2 \quad (4)$$

where C_i, is the measured data point at time i, n = 24 (h).

Equation 4 is a measure of quality of fit for Equation 3, and is important for investigating the diurnal deviations of cosmic ray intensity. Figure 1 illustrates the monthly square diurnal variation with the fit of the first harmonic.

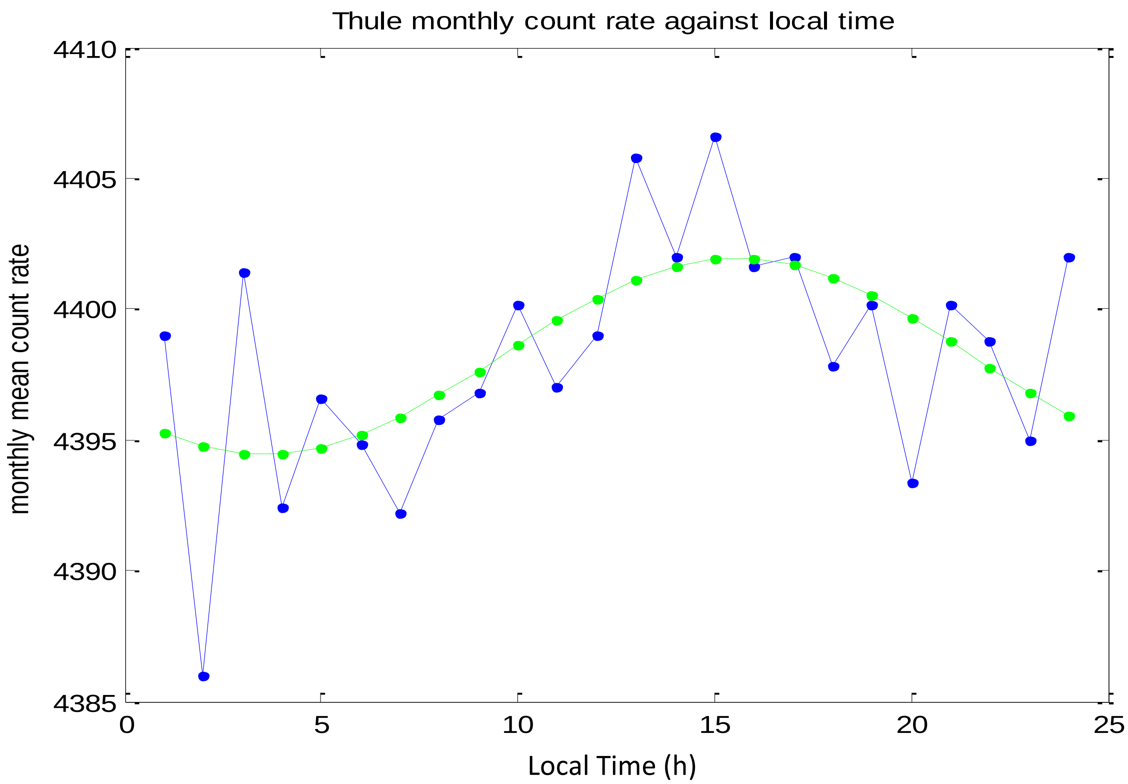

Figure 1. Illustration of solar quiet day diurnal variation with the fit of the first harmonics.

The count rates for all stations were normalized such that the value of the mean of October, 2007 was 100%. This is to reduce the effect of the differences in the instrument from one station to the other. The profile of the monthly mean count rates is shown in Figure 2.

The monthly mean of the daily sunspot number and aa index were obtained, representing solar activity and geomagnetic activity, respectively. Their linear correlations with the monthly mean count rate and amplitude were obtained. The correlation coefficient r_{xy} between two independent variables x and y is given by Equation 5.

$$r_{xy} = \frac{\sum_{i=1}^{n}(x_i - \bar{x})(y_i - \bar{y})}{\sqrt{\sum_{i=1}^{n}(x_i - \bar{x})^2} \cdot \sqrt{\sum_{i=1}^{n}(y_i - \bar{y})^2}} \quad (5)$$

Where: n is number of variables, $\bar{x}$ = mean of x dataset (that is, x_1, x_2…..x_n), $\bar{y}$ = mean for y dataset (that is, y_1, y_2…..y_n).

These correlations were obtained at 0.05 significance level. Student T-test (Equation 6) was carried out to determine the significance of the correlations.

$$T = \frac{\overline{X}_1 - \overline{X}_2}{\sqrt{\frac{S_1^2}{n_1} + \frac{S_2^2}{n_2}}} \quad (6)$$

$\overline{X}_1$ = Mean of first dataset.
$\overline{X}_2$ = Mean of second dataset.
S_1 = Standard deviation of first dataset.
S_2 = Standard deviation of second dataset.
n_1 = Number of values in the first dataset.
n_2 = Number of values on the second dataset.

The partial correlation between two variables x and y, when controlling for the effect of a third variable z is given by Equation 7.

$$r_{xy.z} = \frac{r_{xy} - r_{xz} r_{yz}}{\sqrt{(1 - r_{xz}^2)(1 - r_{yz}^2)}} \quad (7)$$

Where r_{xy}, r_{xz}, and r_{yz} are the respective correlation coefficients between x and y, x and z, and y and z.

To understand the solar cycle dependency of the phase of the quiet day diurnal flux, the period 1981 to 2007 was divided into 5 periods vis; Solar minimum 1 = phase hours of (1985 + 1986 + 1987); Solar minimum 2 = phase hours of (1995 + 1996 + 1997); Solar minimum 3 = phase hours of (2006 + 2007); Solar maximum 1 = phase hours of (1988 + 1989 + 1990); Solar maximum 2 = phase hours of (1999 + 2000 + 2001). It is expected that any solar cycle dependent variation in phase will show as a shift in the phase.

RESULTS AND DISCUSSION

The time series plots of monthly percentage count rate and amplitude for each station are presented in Figures 2 and 3, respectively. Figure 4 shows the time series plot of the dispersion observed from the transformed data. The dispersion is a measure of how much the fit deviates from

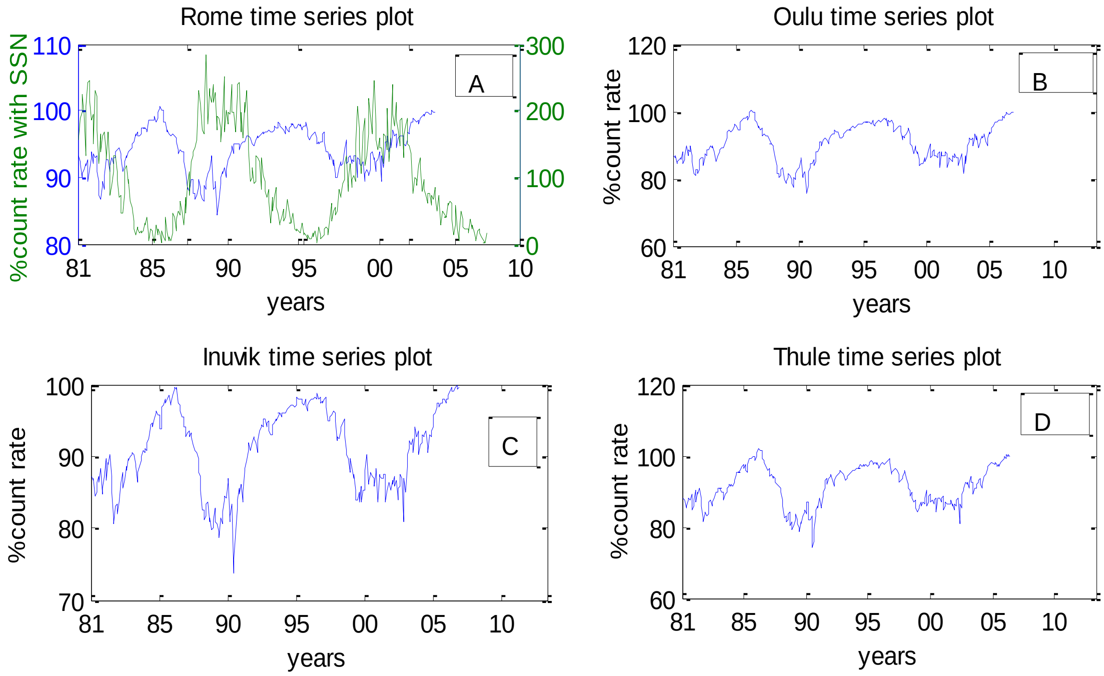

Figure 2. Time series of the monthly mean count rates (1981 to 2007) for A- Rome Station, B- Oulu Station, C-Inuvik Station, and D- Thule Station. Figure 1A is superposed with monthly mean of sunspot number.

Table 2. Inter-station monthly mean count rates correlations**.**

Station	Thule	Inuvik	Oulu	Rome
Thule	1	0.99	0.97	0.97
Inuvik		1	0.97	0.98
Oulu			1	0.96
Rome				1

Table 3. Inter-station amplitude correlations.

Station	Thule	Inuvik	Oulu	Rome
Thule	1	0.47	0.49	0.41
Inuvik		1	0.57	0.57
Oulu			1	0.7
Rome				1

the complex wave form. The time series plot of sunspot number have been superimposed on the time series plot of Rome in Figure 2A. Tables 2, 3 and 4 show the inter-station correlation for mean, amplitude and dispersion, respectively. Tables 5 and 6 show the respective mean and amplitude correlation with sunspot number and aurora indices for all stations.

The amplitude and phase of quiet time (monthly) mean of the diurnal wave of cosmic ray flux received at four neutron monitor stations has been analysed. The amplitude of the diurnal variation is the maximum displacement obtained after Fourier analysing the discrete dataset, t, while the phase refers to the particular hour of the maximum displacement. The interest here is to study the trends and features of the cosmic ray solar quiet day variations and their associations with solar and geomagnetic activities. To achieve this, cosmic ray count rate data from the cosmic ray neutron monitor stations

Table 4. Inter-station dispersion correlations.

Station	Thule	Inuvik	Oulu	Rome
Thule	1	0.19	0.25	0.12
Inuvik		1	0.3	0.24
Oulu			1	0.41
Rome				1

Table 5. Geomagnetic activity index (aa) and sunspot number correlation (and partial correlation) with the monthly mean count rates of all four stations.

Mean	SSN	aa index (SSN removed)
Thule	-0.81	-0.56 (-0.46)
Inuvik	-0.82	-0.58 (-0.50)
Oulu	-0.79	-0.57 (-0.46)
Rome	-0.81	-0.56 (-0.45)

Table 6. Geomagnetic activity index (aa) and sunspot number correlation (and partial correlation) with the amplitude of all four stations.

Station	SSN	aa index (SSN removed)
Thule	0.18	0.20 (0.14)
Inuvik	0.14	0.14 (0.10)
Oulu	0.06	-0.06 (-0.04)
Rome	0.20	0.17 (0.10)

has been subjected to harmonic analysis and the time series of the monthly mean, amplitude and dispersion have been obtained. In addition, the phase distributions of the stations diurnal wave have been obtained and are discussed here.

Figure 2 shows the monthly mean count rate (in percentage normalized to the value of October, 2007) of the four stations. The figure shows the classical inverse association of cosmic ray count rates with solar activity as can be seen in Figure 2A; low count rate during solar maxima (1988 to 1990, 1999 to 2001) and higher count rates during solar minima (1985 to 1987, 1995 to 1997, 2006 to 2007); which agrees with Balasubrahmanyan (1968). The sharp peak followed by broad peak after eleven (11) year interval (1985 to 1995) is a validation of the method used and is consistent with the twenty-two (22) year solar activity cycles as reported in earlier works (Hester et al., 2002; Okpala and Okeke, 2011; Kudela and Sabbah, 2016).

Figure 3 show strikingly similar temporal variations for all stations with mid-latitude and aurora region stations (Rome and Inuvik) showing more dramatic spatial variation during the solar maxima periods (6A and 6C). The troughs (solar maxima) are usually associated with multiple peaks. The peaks of aurora station (Inuvik) and mid-latitude station (Rome) during solar maxima are more intense than the peaks at Thule and Oulu. The Inuvik NM showed strong variability in the monthly mean profiles especially during the solar maximum period while retaining the general trend of decreases during solar maximum and increased count rate during solar minimums. The quiet time monthly mean values of the normalized CR flux for the four stations generally show similar trends which suggest a common source of modulation.

The amplitude of the diurnal variation did no show similar profiles for all the stations and certainly did not exhibit solar activity dependence. The reason for this could be related to different local forcing for the stations studied. Tables 2 and 3 show the inter-station correlation for the monthly mean count rate and amplitude. Very strong association was observed for the monthly mean count rate of the four stations, ranging from 0.96 to 0.99. We equally observed moderate correlations ranging from 0.47 to 0.70 for the inter-station amplitude correlation. These correlations were significant at 0.05 significant

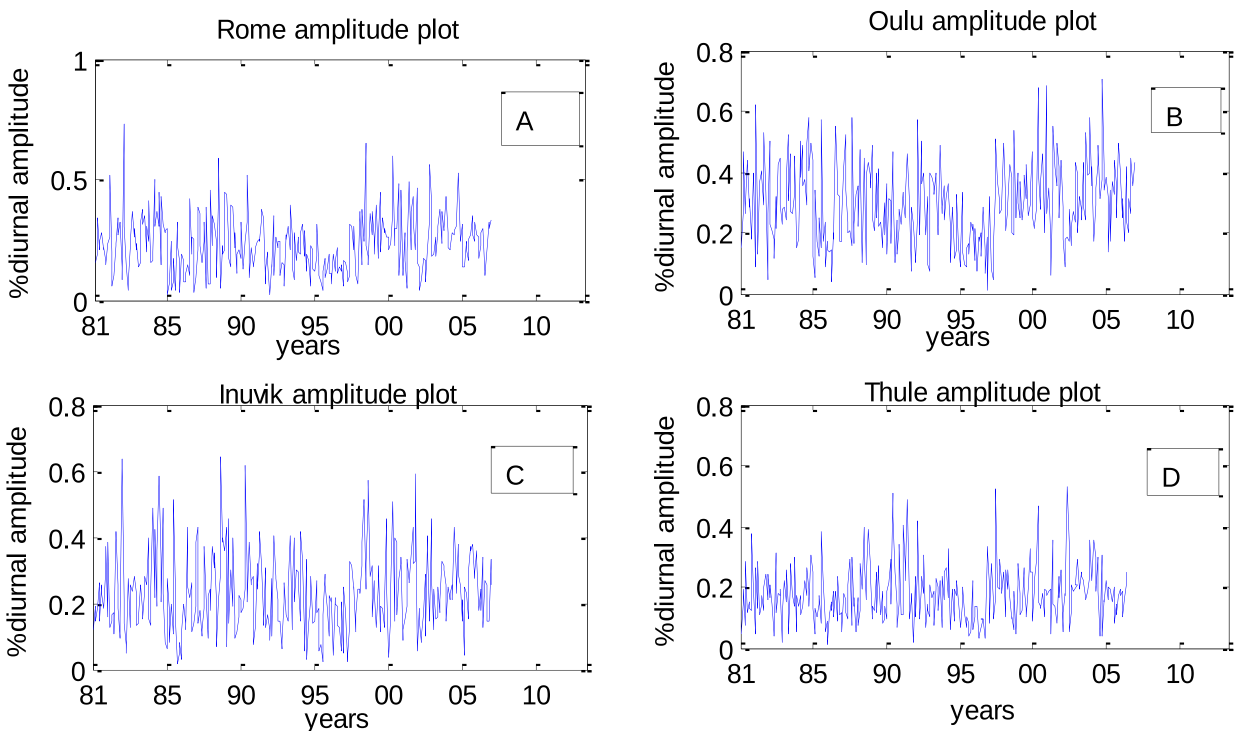

Figure 3. Time series of the mean percentage diurnal amplitude of CR flux (1981 to 2007) for A- Rome Station, B Oulu Station, C-Inuvik Station, and D- Thule Station.

levels. Tables 5 show the correlation between the monthly mean count rate and sunspot number/geomagnetic activity, while Table 6 shows the correlation between amplitude and sunspot number/geomagnetic activity index (aa) for all stations. The geomagnetic activity index correlated negatively and fairly well with monthly mean count rate for all stations. Removing the effect of solar activity (SSN) on their association showed a decrease in the value of their correlation but it was not sufficient to infer that the original association was spurious. The aa-index correlated weakly with the amplitude. The negative correlation between cosmic rays count rate and SSN has been well established and simply validates the method used in obtaining the parameters. Hence, the correlation obtained in Table 5 which is generally greater than 0.45 at 95% confidence, suggests that the geomagnetic activity affects the mean values of the count rates in spite of the solar activity modulation. There was no evidence to suggest that the cut off rigidity of the stations played a strong role in this consideration (comparing Thule and Rome correlation with aa index).

The dispersion is a measure of how the NM count rate deviated from the transformed data. Figure 4 shows the time series plots of the dispersion for the four stations. It is evident that there is similarity between the profiles of Oulu and Rome stations; showing sharp dispersions close to 1989 and 2003. Inuvik and Thule showed lesser dispersion. Solar maxima periods are more dispersed. Inter-station dispersion correlation was poor. Rome and Oulu showed greater dispersion correlation (with 0.41) as can be seen in Table 4. These observations may be an indication that the dispersion could be more affected by rigidity of the individual stations than earlier thought. However, more analysis is required to better understand these observations. In addition, it is suggested here that during high solar activity, the variation of the high latitude stations could be affected by the funnelling of low energy solar cosmic rays through the cusps to the surface.

Charts showing the frequency of phase time (ϕ_n) for each station used are presented in Figure 5. Rome had a range of phase time between 12th to 16th h with the highest frequency of occurrence in the 14th h. Oulu similarly had varying phase time between 15th to 18th h with the highest frequency of occurrences in the 16th and 17th h. This was similar to our observation in Inuvik which had phase time between 13th to 18th h with the highest frequency of occurrences in the 16th and 17th h. Thule highest frequency of occurrences was in the 14th and 15th h.

To study the solar activity dependent features of the phase time, we grouped the years used in the study into solar maxima and minima periods. The frequencies of the phase time for the various stations are displayed in Figures 6 to 9. Summary of the profiles of the histograms in Figures 6 to 9 is presented in Table 7.

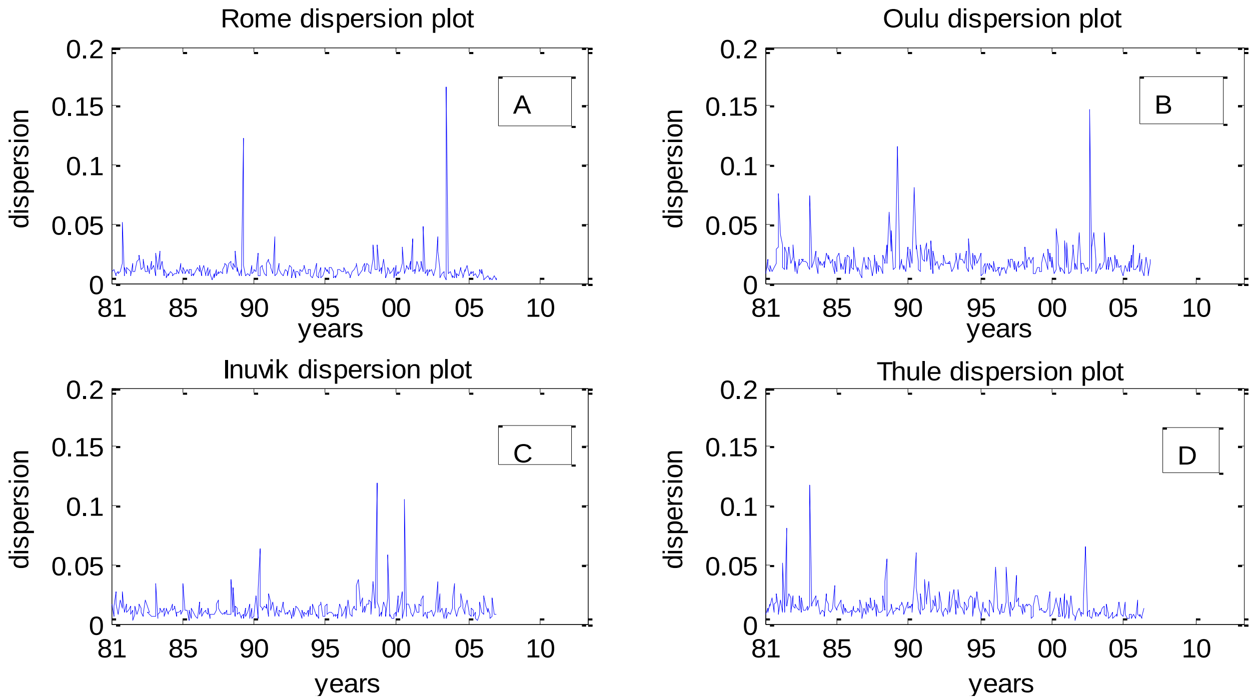

Figure 4. Time series of the mean dispersion of CR flux (1981 to 2007) for A- Rome Station, B Oulu Station, C-Inuvik Station, and D- Thule Station.

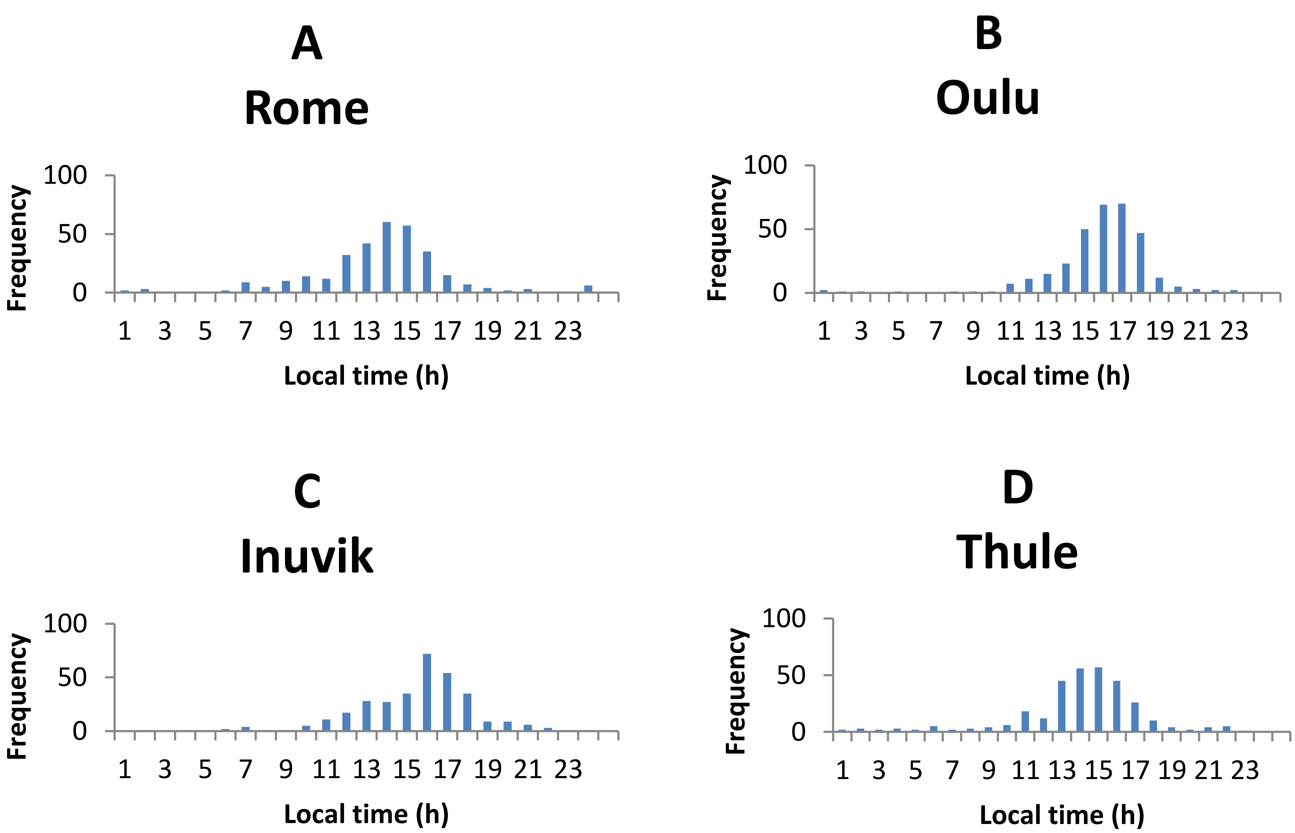

Figure 5. Chart showing frequency of different phase (times) for the stations. A- Rome Station, B- Oulu Station, C- Inuvik Station, and D- Thule Station. The phase used here was obtained using all the months from 1981 to 2007.

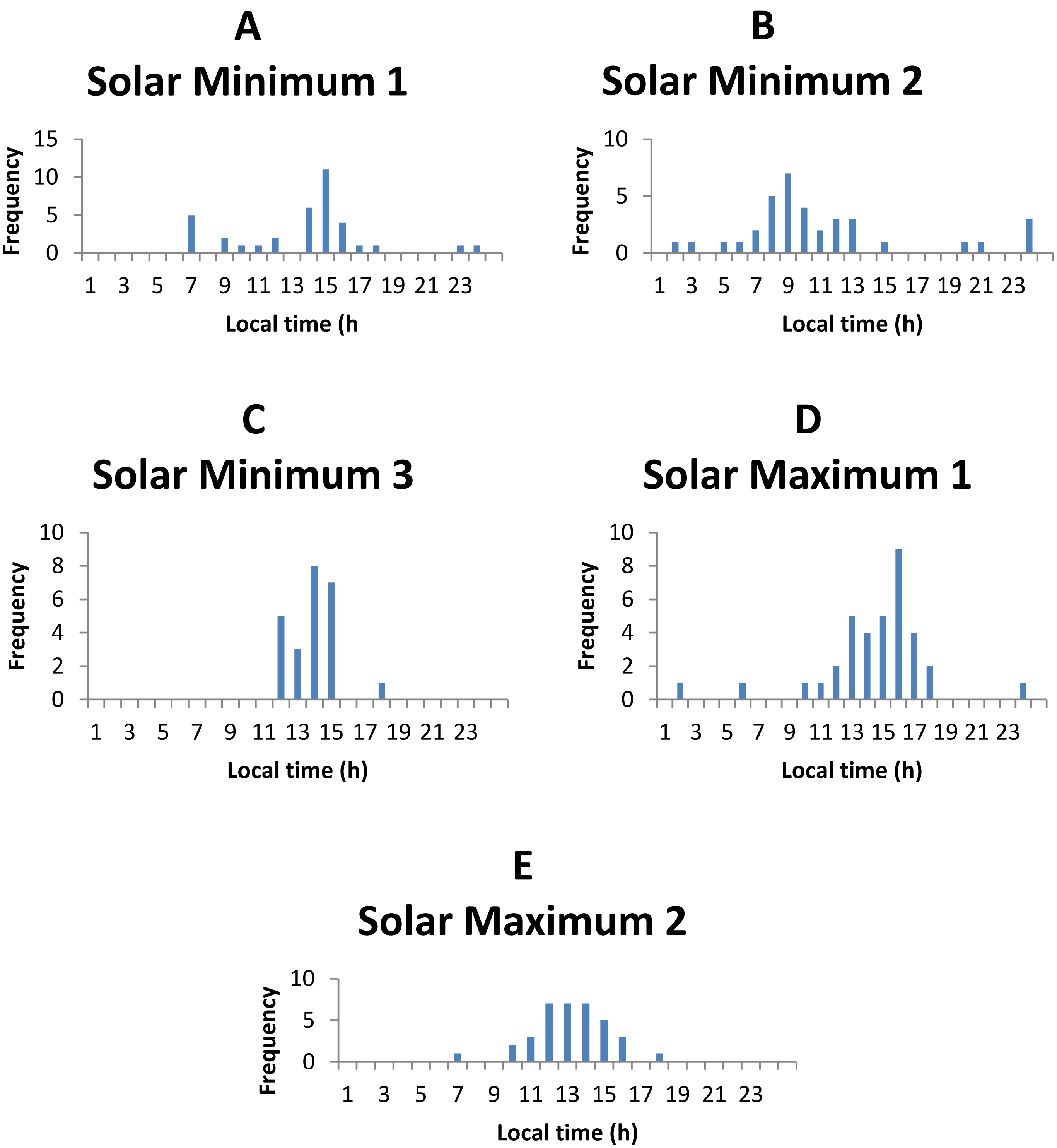

Figure 6. Chart showing frequency of different phase (times) for the Rome Station. A- Solar minimum 1 and was calculated using years 1985, 1986 and 1987; B- Solar minimum 2 and was calculated using 1995, 1996, 1997; C- Solar minimum 3 and was calculated using 2006 and 2007; D- Solar maximum 1 which was calculated using 1988, 1989 and 1990; while E- Solar maximum 2 calculated using data from the years 1999, 2000 and 2001.

From Table 7, comparing solar minima 1, 2 and 3, it was observed that solar minima 1 and 3 have very close phase time for all the stations. Solar minimum 2 phase time is earlier when compared to solar minima (1 and 3). The

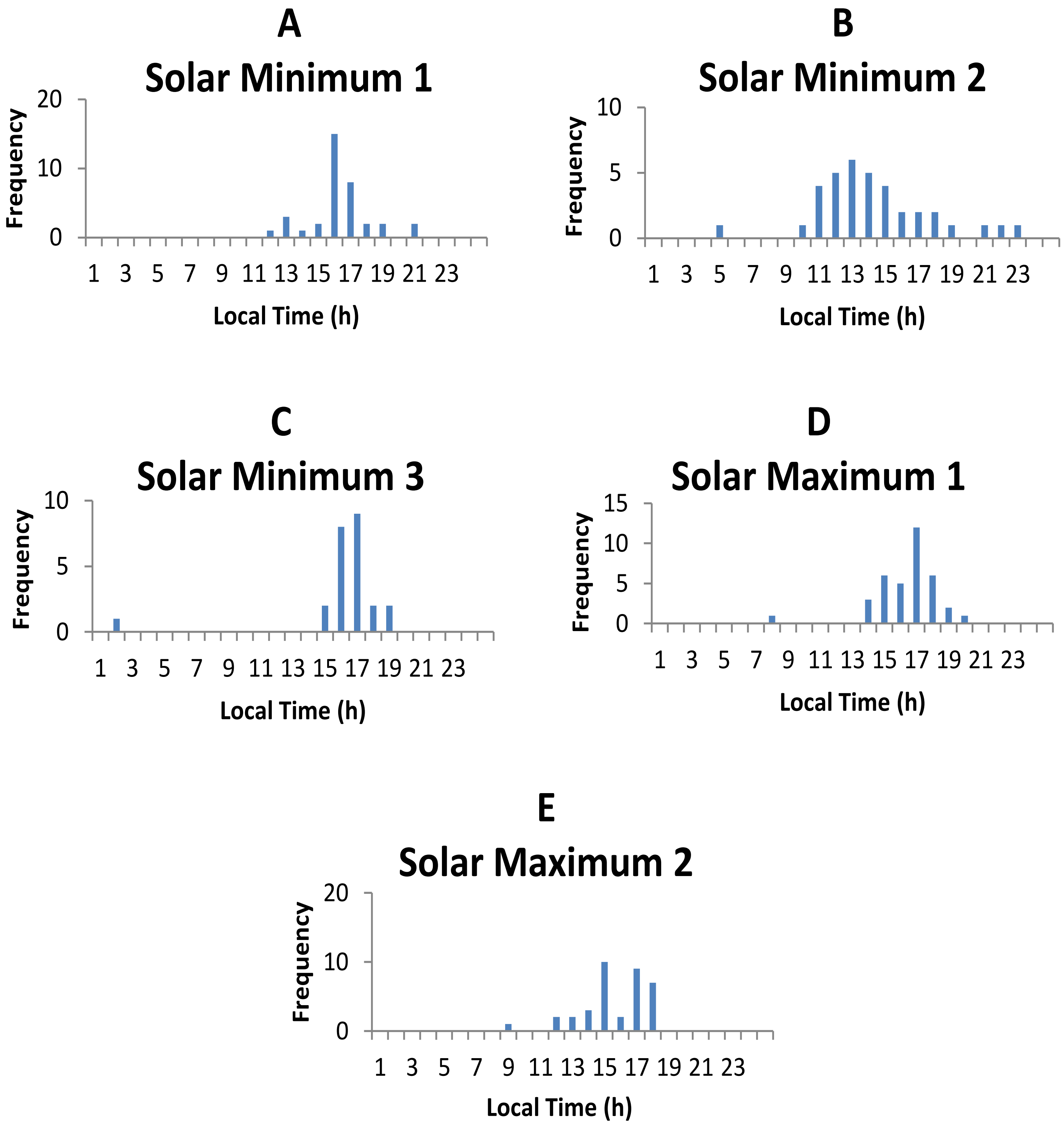

Figure 7. Chart showing frequency of different phase (times) for the Oulu Station. A- Solar minimum 1 and was calculated using years 1985, 1986 and 1987; B- Solar minimum 2 and was calculated using 1995, 1996, 1997; C- Solar minimum 3 and was calculated using 2006 and 2007; D- Solar maximum 1 which was calculated using 1988, 1989 and 1990; while E- Solar maximum 2 calculated using data from the years 1999, 2000 and 2001.

difference here could be because of the sharp and broad peak nature of these cycles caused primarily by pole reversal of the magnetic field of the sun. For solar maximum 1 and solar maximum 2; we observed that the phase time was quite

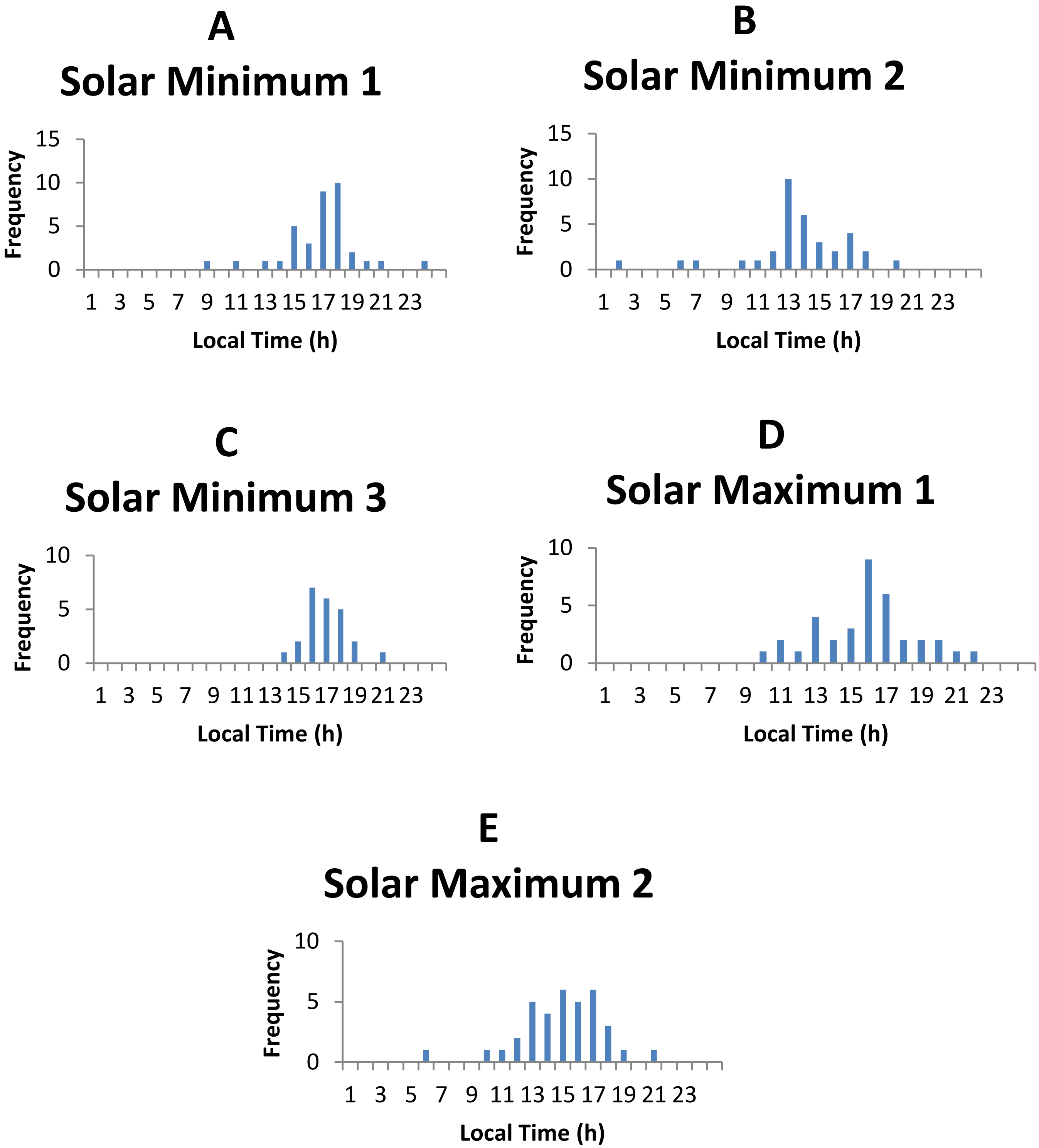

Figure 8. Chart showing frequency of different phase (times) for the Inuvik Station. A- Solar minimum 1 and was calculated using years 1985, 1986 and 1987; B- Solar minimum 2 and was calculated using 1995, 1996, 1997; C- Solar minimum 3 and was calculated using 2006 and 2007; D- Solar maximum 1 which was calculated using 1988, 1989 and 1990; while E- Solar maximum 2 calculated using data from the years 1999, 2000 and 2001.

close with solar maximum 2 coming slightly earlier than solar maximum 1. This shows that the phase time follows a twenty-two (22) year variability pattern thereby giving credence to the solar modulation of cosmic rays count rates.

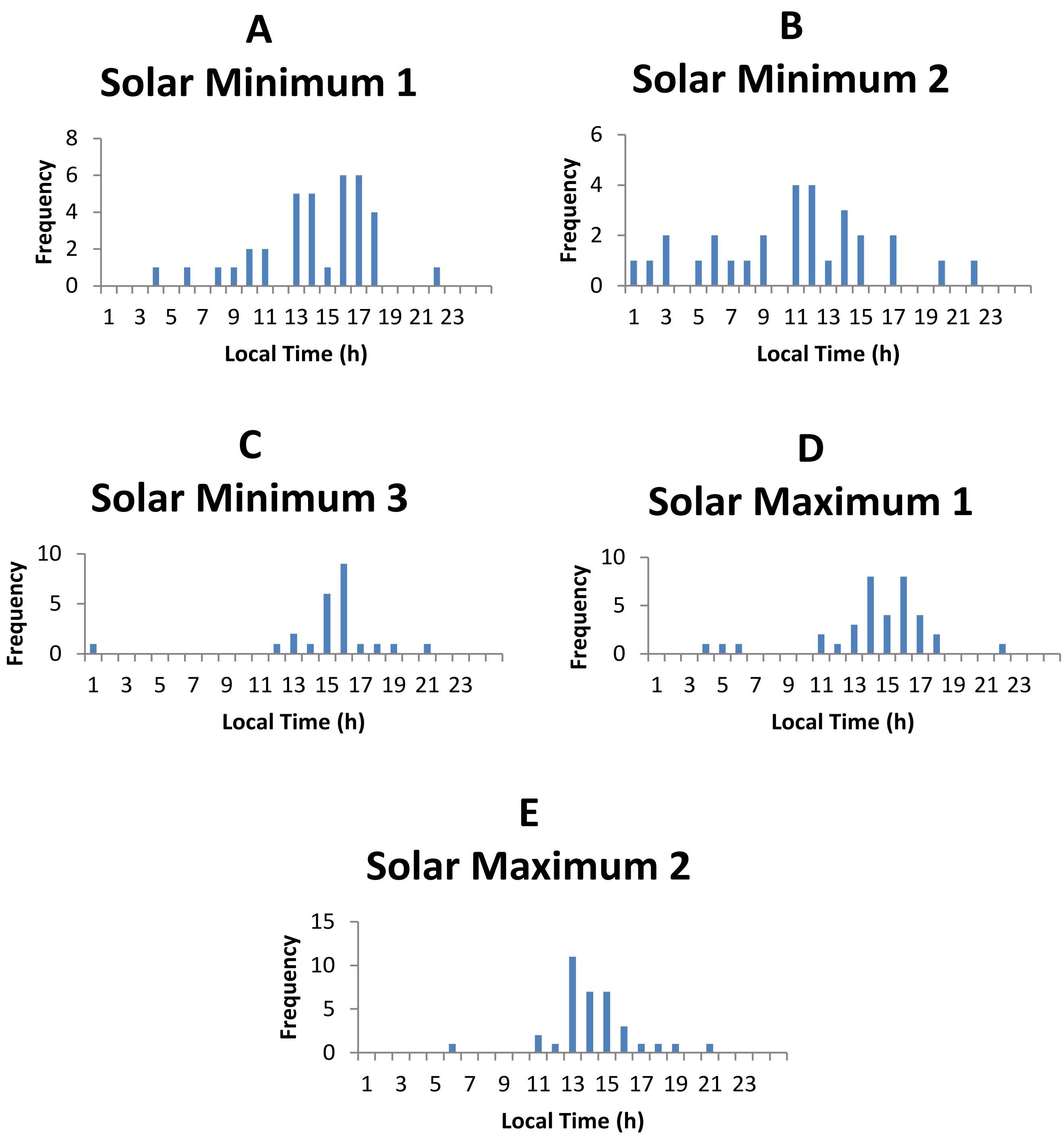

Figure 9. Chart showing frequency of different phase (times) for the Thule Station. A- Solar minimum 1 and was calculated using years 1985, 1986 and 1987; B- Solar minimum 2 and was calculated using 1995, 1996, 1997; C- Solar minimum 3 and was calculated using 2006 and 2007; D- Solar maximum 1 which was calculated using 1988, 1989 and 1990; while E- Solar maximum 2 calculated using data from the years 1999, 2000 and 2001.

Conclusion

In this work, we have studied the features and properties of cosmic ray (CR) diurnal wave on quiet days to identify their dependence on solar and geomagnetic activities. Four stations (one mid-latitude station, one high latitude station with two aurora region stations) have been employed for this work. The data used covered two and half (2½) solar cycles. The following conclusions were made from the results obtained in this study:

Table 7. Stations phase frequency records around solar minimum and maximum periods.

Rome		Oulu		Inuvik		Thule	
Solar cycle	**Most occurring phase hour(s)**	**Solar cycle**	**Most occurring phase hour(s)**	**Solar cycle**	**Most occurring phase hour(s)**	**Solar cycle**	**Most occurring phase hour(s)**
Solar minimum 1	15	**Solar minimum1**	16	**Solar minimum 1**	17 & 18	**Solar minimum 1**	16 & 17
Solar minimum 2	9	**Solar minimum 2**	12, 13 & 14	**Solar minimum 2**	13 & 14	**Solar minimum 2**	11 & 12
Solar minimum 3	14 & 15	**Solar minimum 3**	16 & 17	**Solar minimum 3**	16 & 17	**Solar minimum 3**	15 & 16
Solar maximum 1	16	**Solar maximum 1**	17	**Solar maximum 1**	16 & 17	**Solar maximum 1**	14 & 16
Solar maximum 2	12, 13 & 14	**Solar maximum 2**	15 & 17	**Solar maximum 2**	13, 15 & 17	**Solar maximum 2**	13, 14 & 15

1) The cosmic ray monthly mean count rates in all four stations are highly correlated showing similar temporal variation with marked spatial differences during solar maximum.
2) Quiet-time monthly mean cosmic ray count rate are more associated with solar activity than with geomagnetic activity at both mid and high latitudes. The variability of the amplitude was not associated with either geomagnetic or solar activity in all stations.
3) There was more dispersion during solar maximum period. The diurnal waves of the higher latitude stations (with lesser rigidity) are less dispersive especially during solar active periods.
4) The phase variations tend to follow the twenty-two (22) year solar magnetic activity cycle. It is characterized by a 2 to 6 h change between periods of peak and minimum solar activity.

CONFLICT OF INTERESTS

The authors have not declared any conflict of interests.

ACKNOWLEDGEMENTS

The authors are grateful to the two anonymous reviewers for their very helpful comments towards improvising this paper.

REFERENCES

Agarwal R, Mishra RK (2008). Modulation of cosmic rays at different cutoff rigidity. Braz. J. Phys. 38:108-116.
Ananth AG, Vankatesan D, Pillai S (1993). Long term changes in cosmic ray diurnal anisotropy. Solar Phys. 143:187-196.
Balasubrahmanyan VK (1968). Solar activity and the 11-year modulation of cosmic rays. Solar Phys. 7(1):39-45.
Bazilevskaya BA, Krainev MB, Makhmutov VS, Stozhkov YI, Svirzhevskaya AK, Svirzhevsky NS (1995). The relationship between the galactic cosmic ray intensity and the sunspot distribution. Adv. Space Res. 16(9):221-225.
Belov AV, Gushchina RT, Yanke VG (1999). The spectrum of cosmic rays variations during 19-22 solar cycles. Proc. 26th int. cosmic conf. 7:175-178.
Chillingarian A, Mailyan R (2009). Investigation of diurnal variation of cosmic ray flux in the Beginning of 24th Solar Activity Cycle, proceedings of the 31st ICRC, LODZ, 1-4.
Firoz KA (2008). On cosmic ray diurnal variations: Disturbed and Quiet days, WDS'08 proceedings of contributed papers, part II, 183-188.
Helen M, Evangelos P (2012). Long term cosmic ray variability and the CME-index. Adv. in Astron. pp. 1-8.
Hester J, David B, George B, Ronald G, Bradford S, Howard V, Gary W (2002). 21st Century Astronomy. New York NY: WW Norton & company inc. publishers.
Kane RP (2009). High amplitude anisotropic events (HAE) in cosmic ray diurnal variation during solar cycle 23. Indian J. Radio Space Phys. 38:189-196.
Kudela K, Firoz KA, Langer RD, Kollir V (2008). On diurnal variation of cosmic rays: statistical study of neutron monitor data including Lommicky slit. Proc. 21st Eur. cosmic ray conf. 374-378.
Kudela K, Sabbah I (2016). Quasi-periodic variations of low energy cosmic rays. Sci. China Tech. Sci. 59(4):547-557.
Kumar S, Shrivastava SK, Dubey SK, Richaria MK, Gulati U (1998). Effect of solar poloidal magnetic field reversal on diurnal anisotropy of cosmic ray intensity on quiet days. Indian J. Radio Space Phys. 27:236-240.
Okpala KC, Okeke FN (2011). Investigation of diurnal and seasonal galactic cosmic ray variation on quite days in two mid latitude stations. Astropart. Phys. 34:878-885.
Okpala KC, Okeke FN, Ugwoke AI (2015). Cosmic ray modulation in high and middle latitudes during solar cycles 22 and 23. Can. J. Phys. 93(1):100-104.
Pomerantz MA, Duggal SP (1971). The cosmic ray solar diurnal anisotropy. Space Sci. Rev. 12:75-130.
Sabbah I (2007). Twenty-seven day variation of galactic cosmic rays. Solar Phys. 245:207-217.
Sabbah I, Kudela K (2011). Third harmonic of the 27 periodicity of galactic cosmic rays: coupling with interplanetary parameters. J. Geophys. Res. Space Phys. 116(A4):2156-2202.
Singer SF (1952). Cosmic rays and the sun's magnetic field: Diurnal variation of cosmic rays and the sun's magnetic field. Nature 170:63-64.
Singh Y, Badruddin P (2015). Solar rotational oscillation and its harmonics in the solar wind, geomagnetic and cosmic ray particles during the last two solar minima. Astrophys. Space Sci. 359:60.
Thomas S, Owens M, Lockwood M, Owen C (2017). Decadal trends in the diurnal variation of galactic cosmic rays observed using neutron monitor data. Ann. Geophys. 35:825-838.
Tiwari RK, Achyut P, Pankaj KS, Sushil KS (2011). Relationship of cosmic rays with solar and geomagnetic activity. Ind. J. Sci. Res. 2(4):15-19.
Usoskin IG, Kalevi M (2001). Heliospheric modulation of cosmic rays and solar activity during the maunder minimum. J. Geophys. Res. 106(A8):16039-16046.

academicJournals

Vol. 12(22), pp. 308-321, 30 November, 2017
DOI: 10.5897/IJPS2017.4684
Article Number: C5EF15666744
ISSN 1992 - 1950

http://www.academicjournals.org/IJPS

International Journal of Physical Sciences

Full Length Research Paper

Investigation on equinoctial asymmetry observed in Niamey Station Center for Orbit Determination in Europe Total Electron Content (CODG TEC) variation during ~ solar cycle 23

Ouattara F.[1*], Zerbo J. L.[1,2], Kaboré M.[1,2] and Fleury R.[3]

[1]Laboratoire de Recherche en Energétique et Météorologie de l'espace (LAREME), Université Norbert Zongo, BP 376, Koudougou, Burkina Faso.
[2]Université Nazi Boni, Bobo Dioulasso, 01 BP 1091 Bobo, Burkina Faso.
[3]Telecom Bretagne, Technopole Brest Iroise, 29239 Brest, France.

Received 30 August, 2017 ; Accepted 29 September, 2017

This is an investigation of equinoctial asymmetry in Total electron content (TEC) variability at Niamey (Latitude: 13° 30' 49.18" N, Longitude: 2° 06' 35.28" E) using the Global Ionospheric Maps model constructed by the Center for Orbit Determination in Europe (CODG model) during solar cycle 23, that is, from year 1999 to year 2009. Niamey Center for Orbit Determination in Europe Total Electron Content (CODG TEC) from 1999 to 2009 show that ionization follows solar cycle and presents semi-annual variation with equinoctial asymmetry. In CODG TEC, generally, March/April maximum density is larger than that of September/October except during years 1999 and 2001. For all years (1999-2008), electronic density is higher between 1400 and 1700 UTC with the maximum at 1400 UTC. On one hand, Ap and aa index via pixel diagram and on the other hand, seasonal and sunspot cycle variation have been used to explain the exception of years 1999 and 2001. It was found that asymmetry of 1999 is due to solar wind particularly to fluctuating wind and asymmetry of 2001 results from CMEs.

Key words: Global positioning system (GPS), Center for Orbit Determination in Europe Total Electron Content (CODG TEC), ionization, asymmetry, equatorial ionosphere.

INTRODUCTION

The equinoctial asymmetry in monthly or seasonal ionospheric parameters such as foF2, NmF2, TEC (Rishbeth et al., 2000; Chakraborty and Hajra, 2008; Ouattara et al., 2012; Naméma and Ouattara, 2013; Hajra et al., 2016) and in geomagnetic activity (Green, 1984; Cliver et al., 2000; 2002; Chakraborty and Hajra, 2010; Hajra et al., 2013) have been intensively investigated and three principal hypotheses or mechanisms are proposed

*Corresponding author. E-mail: fojals@yahoo.fr.

to explain such variation: (1) axial mechanism (Bohlin, 1977) for which the peak occurrence times correspond to those of the maximum of solar B_0 angle (Cliver et al., 2000). This mechanism is also explained by seasonal variation of solar wind speed (Murayama, 1974); (2) equinoctial mechanism (Svalgaard, 1977) where the peak occurrence times are those of the minima of the solar declination (Cliver et al., 2000 and (3) Russell-McPherron mechanism (Russell and McPherron, 1973) where the peak occurrences are due to those of the maximum of solar P angle. The solar B_0 angle corresponds to Earth's heliographic latitude; and the solar P angle is the position angle of the northern extremity of the Sun's rotation axis, measured eastward from the north point of the disk (Cliver et al., 2002).

For the understanding of the response of CODG model in West Africa region, we morphologically analyse CODG TEC time variation from 1999 to 2009 as a function of sunspot number R12. Pixel diagrams were also built with geomagnetic aa and Ap indices. The three mechanisms (Axial, Russell McPherron and equinoctial) were verified for explaining ionospheric semi-annual variation. One of the goals of the present paper is to determine a possible cause of the asymmetry.

MATERIALS AND METHODS

The Total Electron Content (TEC) at Niamey station (Geo Lat 13°28'45.3"N; Geo Long: 02°10'59.5"E) during solar cycle 23 was determined using the model of the coefficients of the ionosphere given by Centre for Orbit Determination in Europe (CODE). The CODE is one of the centres of analysis of International GNSS Service (IGS, http://www.igs.org/network). The Global Ionospheric Maps model constructed by the Center for Orbit Determination in Europe (GIM/CODE or CODG model) is used to get the Total Electron Content. Throughout the paper TEC obtained with the GIM/CODE model is called CODG TEC. The database includes:

(1) CODG TEC computed at Niamey station (Geo Lat 13°28'45.3"N; Geo Long: 02°10'59.5"E) in Niger by using IGS database where IGS means International GNSS (Global Navigation Satellite Systems) Service. These data can be found at http://igscb.jpl.nasa.gov;
(2) Geomagnetic index aa (Mayaud, 1968, 1971, 1972, 1973), taken from SPIDR database (http://isgi.unistra.fr/data_download.php), permits the evaluation of different geomagnetic conditions (quiet and disturbed conditions).
(3) Sunspot number R12 data provided by database http://www.sidc.be/silso/datafiles, gives the different solar cycle phases years.
(4) The planetary index Ap, obtained from NGDC database (http://www.ngdc.noaa.gov), characterizes the geoeffectivity of solar particles (Chapman and Bartels, 1940) from coronal holes (Nolte et al., 1976).

It is well known that there are three types of solar winds (Legrand and Simon, 1989; Simon and Legrand, 1989; Richardson et al., 2000; Richardson and Cane, 2002; Ouattara and Amory Mazaudier, 2009): (1) high stream solar wind speed coming from coronal holes; (2) slow solar wind coming from solar heliosheath and (3) fluctuating solar wind due to the fluctuation of solar neutral sheet.

It can be noted that:

(1) Ap index permits the evaluation of the impact of each type of solar wind (high solar wind speed, slow solar wind and fluctuating solar wind). In fact, this parameter is correlated to solar wind velocity (Snyder et al., 1963; Crooker et al., 1977; Ahluwalia et al., 1994); moreover, it gives a possibility to evaluate the response of the magnetosphere to solar wind inhomogeneity (Dessler and Fejer, 1963); Tsurutani et al. (1995, and references therein) pointed out that Alfvén waves are able to provoke geomagnetic disturbances in high latitudes via their southward magnetic field components. These disturbances are taken into account in the determination of Ap values (Ahluwalia, 2000). The other sources which contribute to the estimation of Ap values are coronal mass ejections (CMEs) (Gosling, 1976; Newkirk et al., 1981) which was first observed by using the coronagraph installed on board The Seventh Orbiting Solar Observatory (OSO-7 satellite) launched on 29 September 1971 (Ahluwalia, 2000).
(2) aa index permits the evaluation of different geomagnetic conditions (quiet and disturbed conditions) and particularly the determination of each class of activity by means of pixel diagrams (Ouattara and Amory-Mazaudier, 2009).

In the present paper, monthly CODG TEC are analysed with attention focused on equinoctial peaks and their asymmetry in order to determine its probable solar sources. This will be done not only by means of pixel diagrams but also by the use of Cliver et al. (2002) results.

RESULTS AND DISCUSSION

Here, the results and analysis were first presented followed by expose of the possible source the peak asymmetry. Figures 1, 2 and 3 give monthly CODG TEC variation from year 1999 to 2007 at Niamey Station. In the top of each panel, red colour shows Ap index monthly variation. In each panel, months are given in abscises axis and universal time calculate (UTC) in ordinates axis. In this figure, TEC is expressed in the unit of 10^{15} el/m^2 (TECU) and colour code starts from blue (corresponding to zero) to red (corresponding to 1400 TECU).

CODG TEC highlights semi-annual variation which is well known in ionosonde data monthly variation. It can be seen in Figures 1, 2 and 3 that the equinoctial maxima and its asymmetry; in general, the maxima of October are superior to those of March except in 1999 and 2001 where it is opposite. Ionization is maximal between 1200 UTC and 1700 UTC with its maximum density at 1400 UTC for all panels. Moreover, it can be noted that on one hand, the intensity of the equinoctial maxima varies with solar cycle (R12) and on the other hand, TEC intensity is correlated with the Ap value.

Figure 4 shows monthly TEC (red) and monthly R12 (blue) evolution from 2000 to 2010 which shows that annual TEC varies with sunspot number; in consequence, annual electronic density can be expressed as a function of sunspot number.

Figure 5 shows season variation of CODG TEC during quiet time characterized by days where aa ≤ 20 nT (panel a) and during disturbed period characterized by aa > 20 nT (panel b). This figure exhibits that the highest peaks appear during solar maximum. This result is consistent with the ionosonde data of Ouagadougou Station as

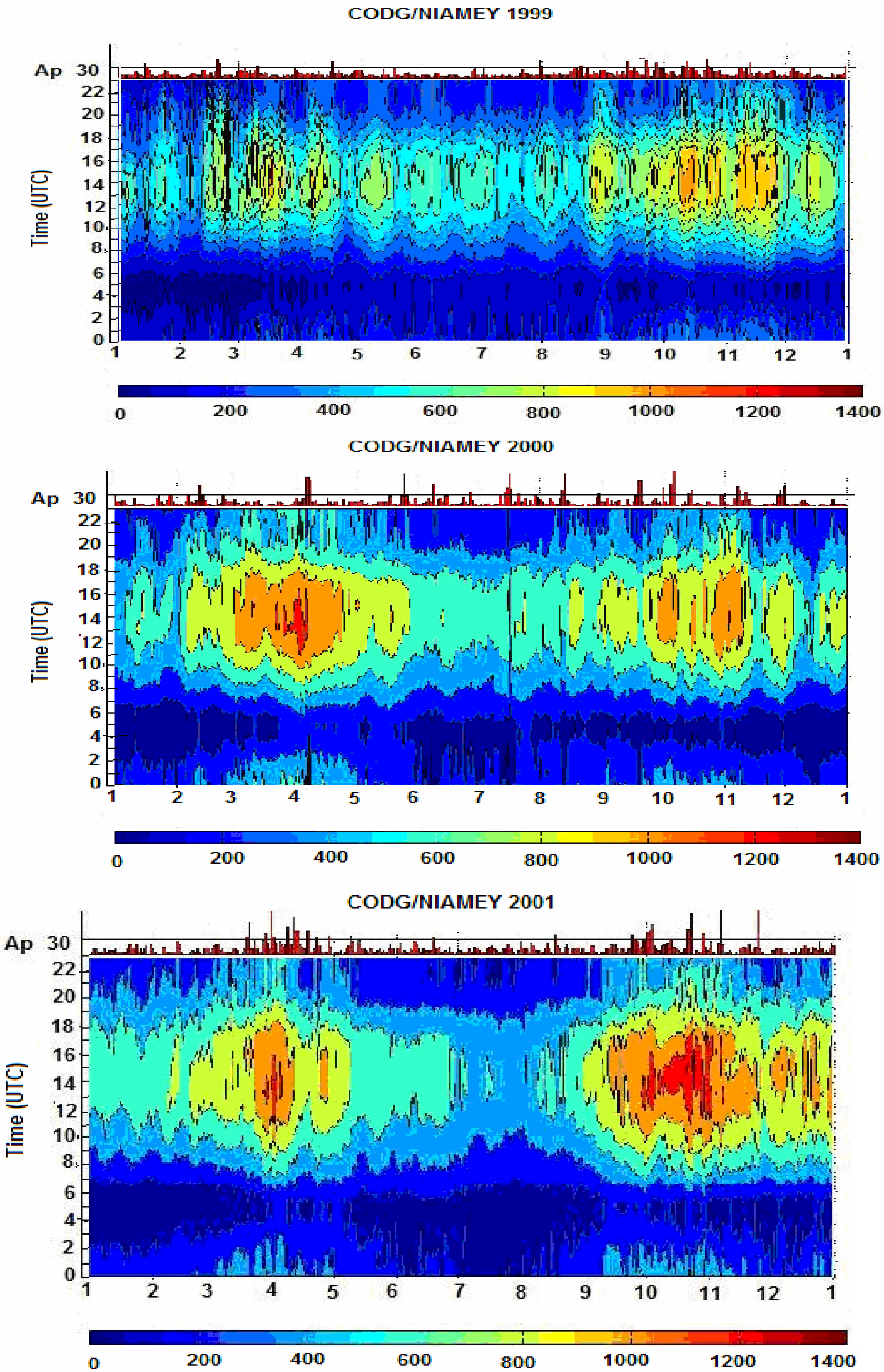

Figure 1. Diurnal CODG TEC evolution from 1999 to 2001.

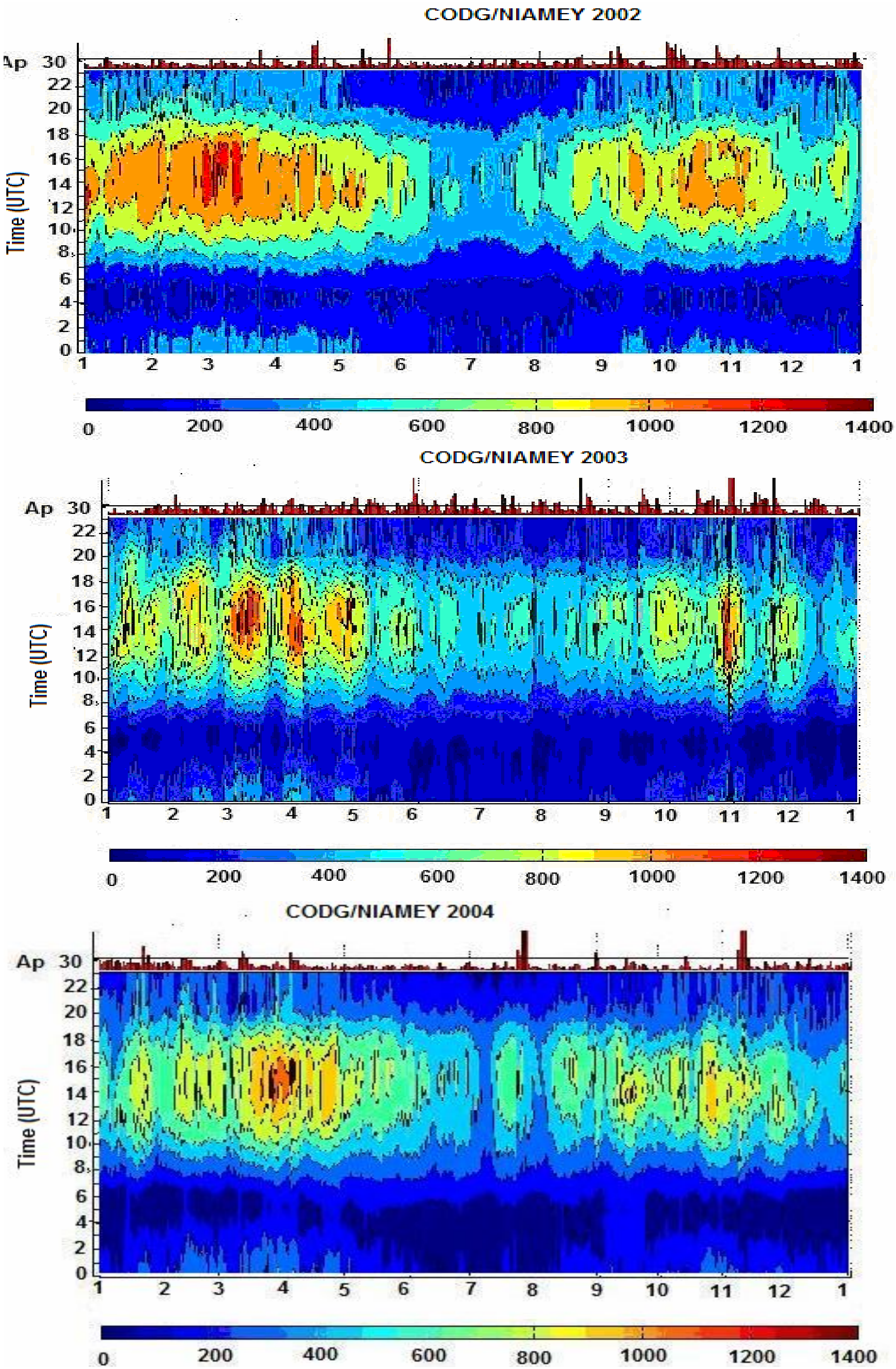

Figure 2. Diurnal CODG TEC evolution from 2002 to 2004.

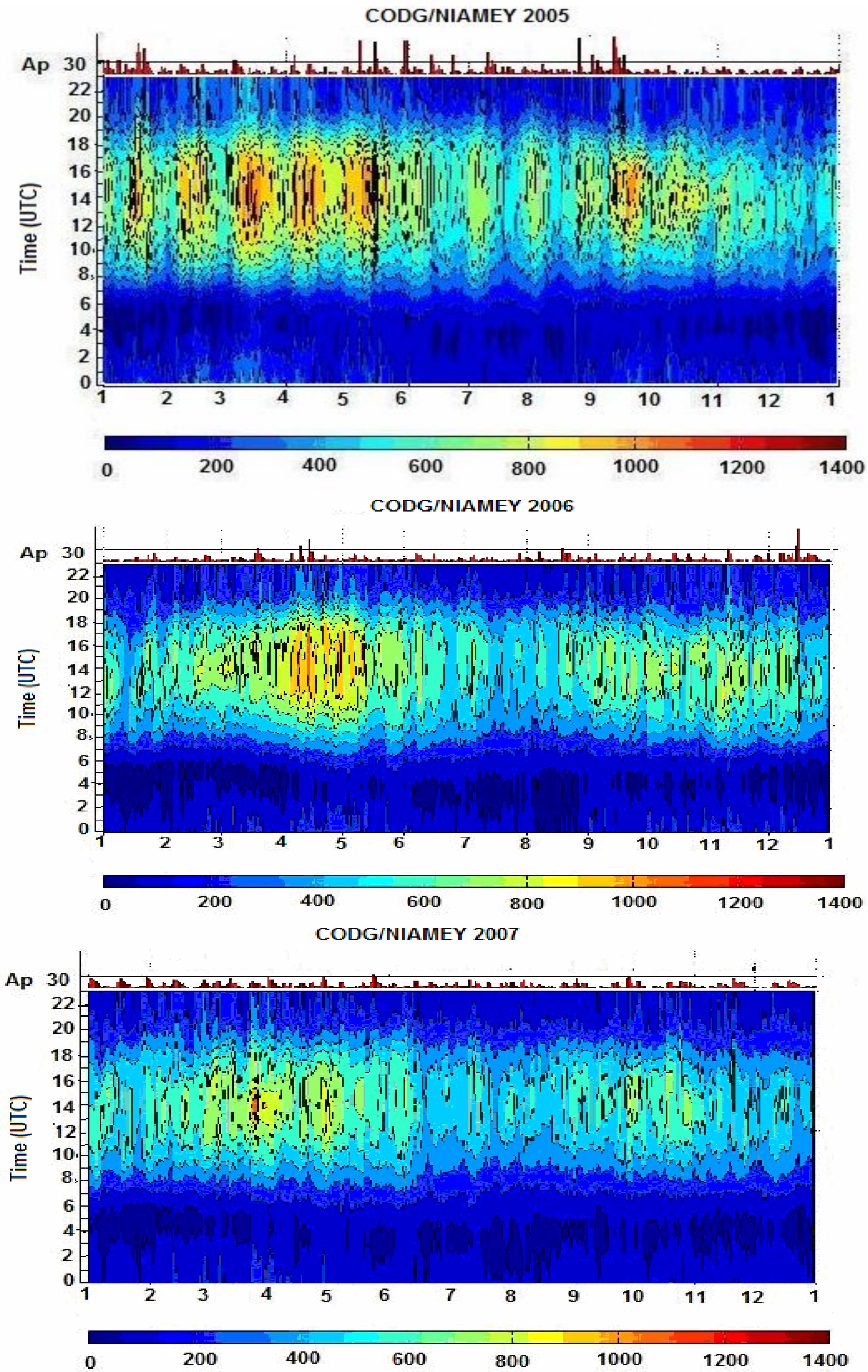

Figure 3. Diurnal CODG TEC evolution from 2005 to 2007.

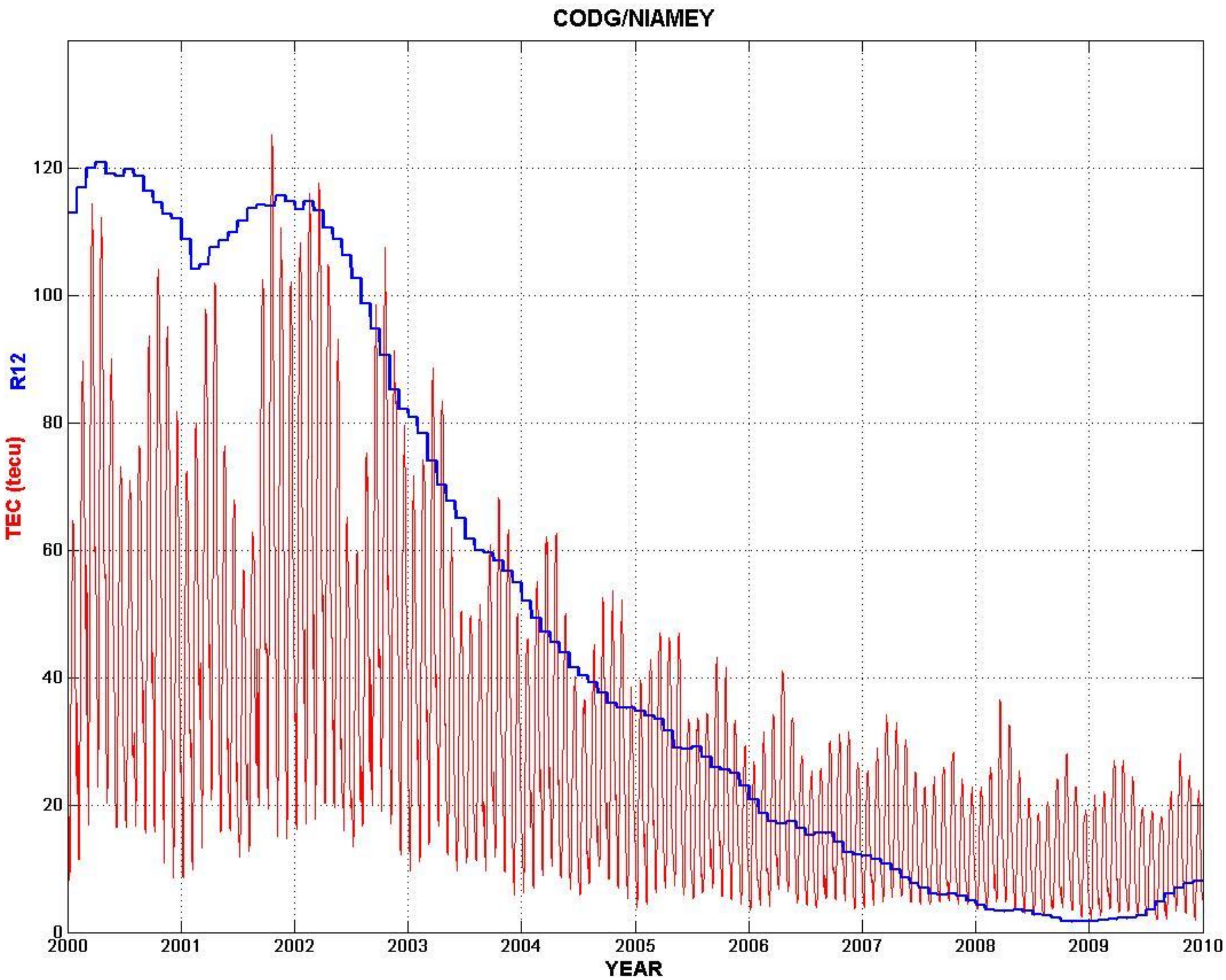

Figure 4. Monthly CODG TEC and R12 variation from 1999 to 2010.

reported by Ouattara et al. (2009). In panel a, one can see the peak asymmetry and March/April peak is higher than that of September/October for all years except these of 1999 and 2001 where it is the opposite. The comparison between results of panels a and b shows that peak amplitude is higher during disturbed period than that of quiet period and the disturbed condition does not modify the asymmetry observed during quiet time.

Analyses of these TEC variations will allow us appreciate (1) the annual variation of the ionosphere and the effect of solar phases on the ionosphere and (2) the impact of solar events on ionosphere.

Possible sources of CODG TEC seasonal asymmetry

To determine the source of CODG TEC asymmetry, sunspot number R12, geomagnetic Ap index, pixel diagrams and the results of Cliver et al. (2002) were used.

a) CODG TEC asymmetry source according to sunspot number

Figure 6 gives seasonal TEC variation at 1200 UT as a function of sunspot number R12 from 1999 to 2008. The green graph concerns local summer season (July month); blue graph is devoted to spring season (March/April); and pink graph highlights autumn season (September/October) TEC variations. Chestnut graph gives winter season (January) TEC variations. Each graph symbol corresponds to one year. From bottom to up, year increases from 1998 to 2007.

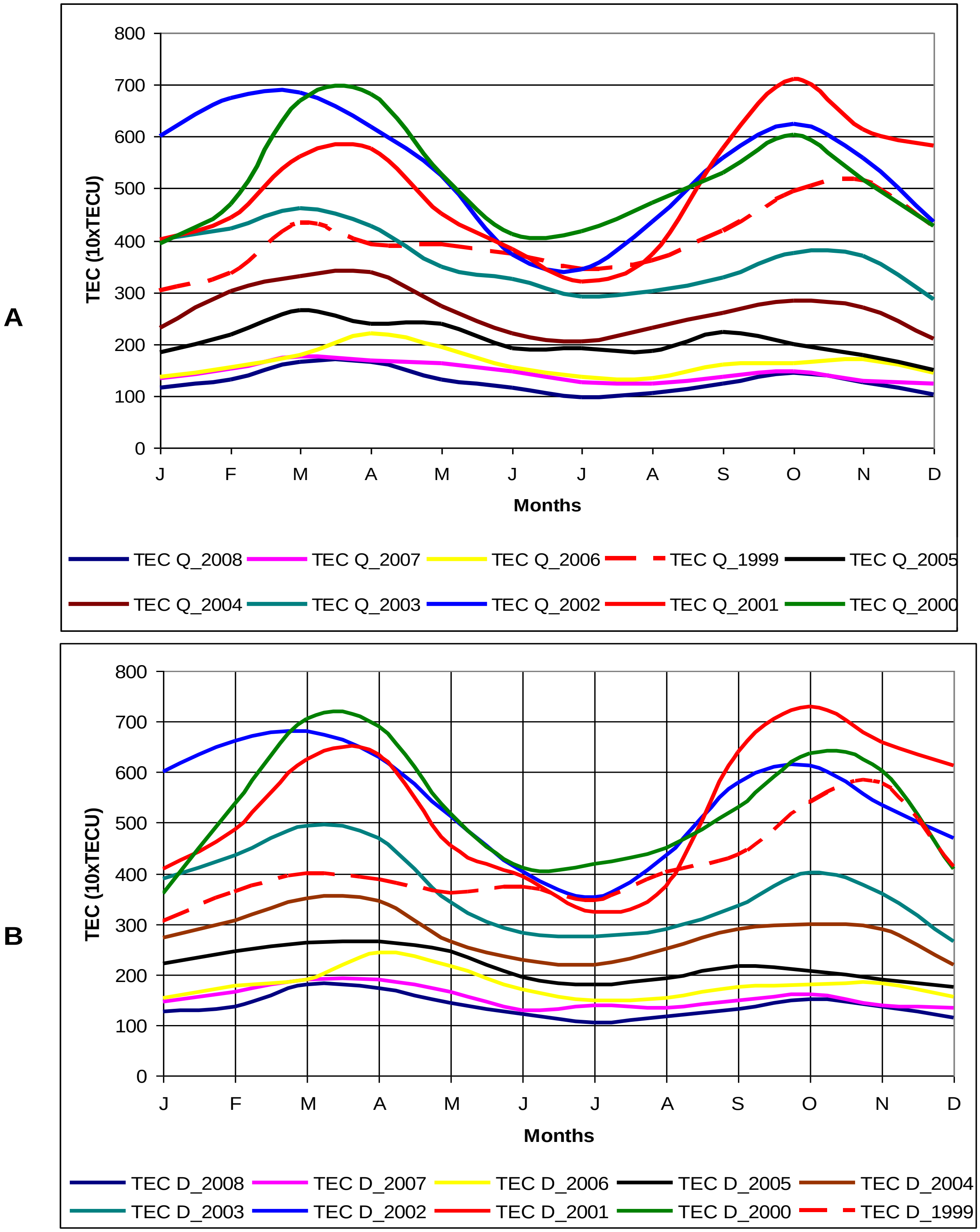

Figure 5. Seasonal CODG TEC variation from 1999 to 2008 during (panel a) quiet days and (panel b) disturbed days.

From Figure 6 it can be concluded that there is linear dependency between seasonal TEC and sunspot number R12. When R12 is less than 96, TEC increases linearly with R12 and the correlation coefficient is in range [0.924, 0.984]. For a given sunspot number, July TEC is the largest than the others. The analysis of Figure 6 exhibits

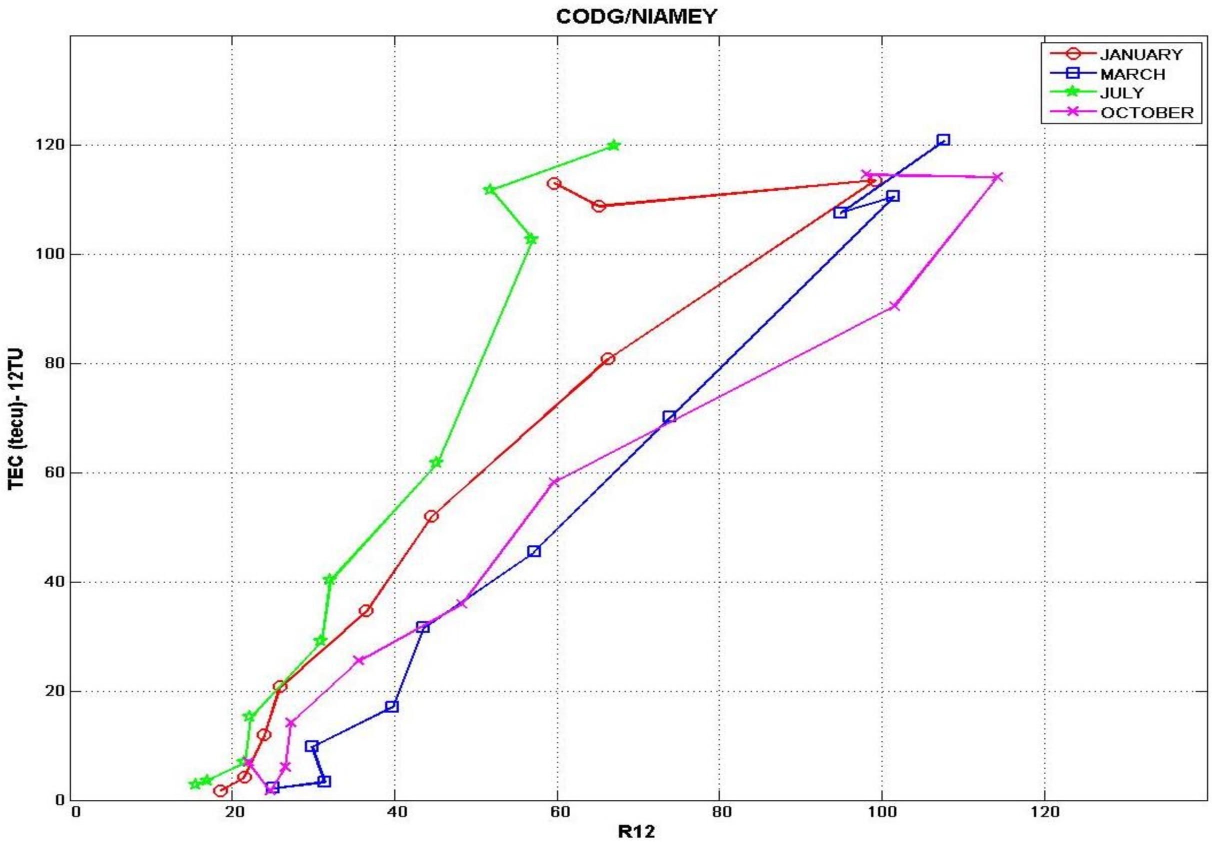

Figure 6. Seasonal CODG TEC variation as a function of sunspot number.

that (1) CODG TEC increases linearly with sunspot number until CODEG TEC is less than 100 TECU, (2) CODG TEC does not show winter anomaly because summer CODG TEC is always larger than that of winter and (3) for R12 = 42, R12 = 76 and R12 = 102 there is no equinoctial asymmetry. For R12 < 42 and 42 < R12< 76, October ionization is larger than that of March and for 76 < R12 < 116 it is the opposite. If only the equinoctial asymmetry results from sunspot, we do have four years (1999, 2000, 2001, 2002) with equinoctial asymmetry anomaly (with respect to the other asymmetry observed during 2003 - 2009) but according to Figures 1, 2 and 3 only two years (1999, 2001) CODG TEC have equinoctial asymmetry anomaly; therefore, we must assert that sunspot is not the only one responsible of such anomaly. To determine the other sources of equinoctial asymmetry anomaly observed during years 1999 and 2001, this research will investigate two ways: (1) utilization of Ap index and (2) employment of pixel diagrams.

We used the planetary index Ap by considering its characteristics notified previously. Pixel diagrams are utilized for permitting the evaluation of the action of different solar events (slow solar wind, solar wind stream, fluctuating solar wind and CMEs) (Legrand and Simon, 1989; Simon and Legrand, 1989; Ouattara, 2009; Ouattara and Amory Mazaudier, 2009).

b) CODG TEC asymmetry source according to Ap index values

Figure 7 presents the two-dimensional monthly CODG TEC variation for year 1999 (Panel a) and year 2001 (Panel b). In year 1999 (Figure 7a) it can be seen that that there is correlation between Ap and CODG TEC during September/October equinox while it is not the same during March/April equinox. Thus, this asymmetry may be due to solar wind by reference of the correlation between Ap index and solar wind as previously indicated. In year 2001 (Figure 7b), the maximum of Ap amplitude arrives at the same time with CODG TEC maximum value during March/April equinox. This situation is not observed during September/October equinox. Therefore, it can be concluded that there is no correlation between Ap and CODG TEC during September/October equinox, whereas the correlation is observed between these two parameters during March/April equinox. Thus, the equinoctial asymmetry observed is not due to solar wind. By reference to parameters which contribute to Ap (as previously indicated), one must conclude that during

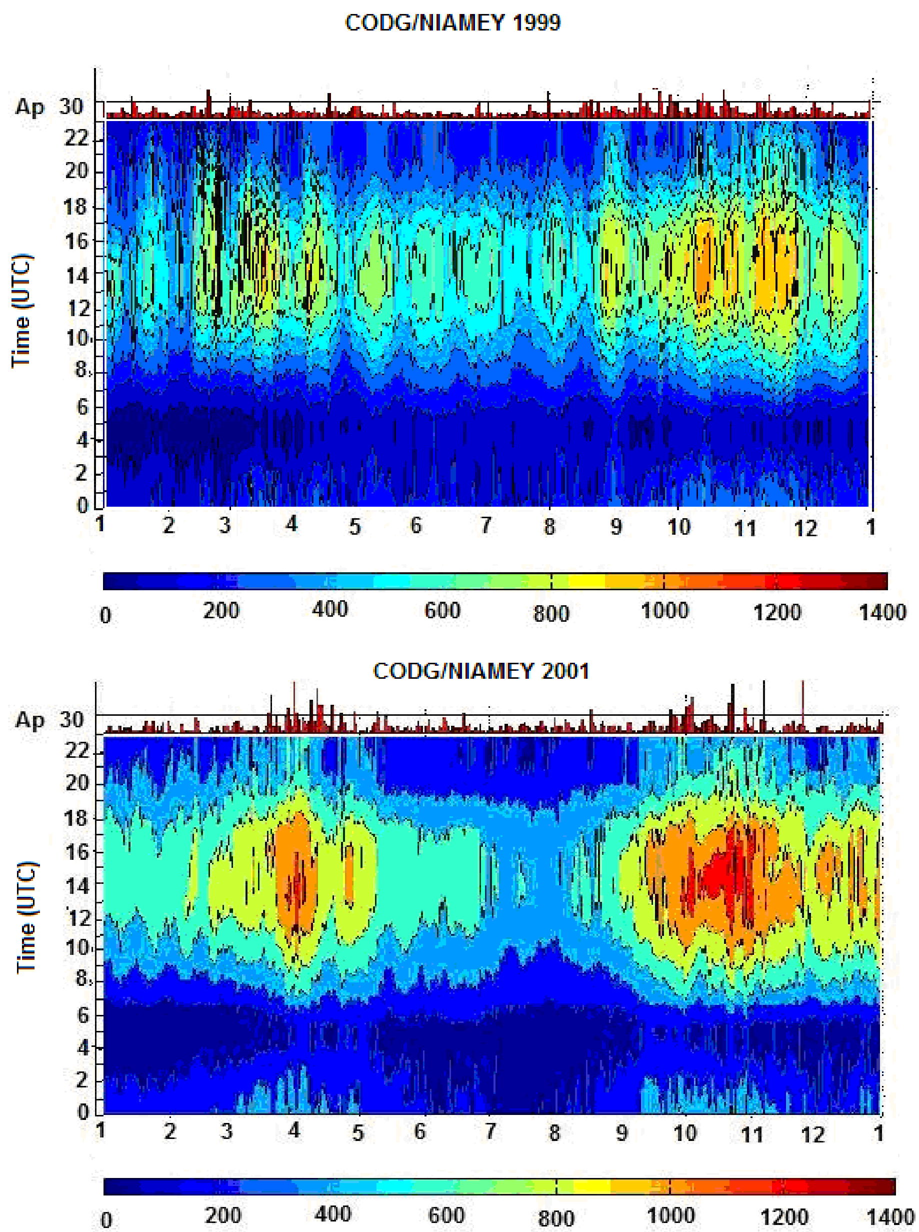

Figure 7. Monthly CODG TEC evolution for year a) 1999 b) 2001.

2001 the equinoctial asymmetry may be provoked by CMEs.

c) CODG TEC asymmetry source according to pixel diagrams

Figure 8 shows pixel diagrams for year 1999 (top panel) and year 2001 (bottom panel). Each line of the pixel shows a 27-day rotation, and successive lines solar rotations. Each number is the daily average of aa index. Shock activity started by non-recurrent sudden storm commencement (SSC) days (http://isgi.unistra.fr/data_download.php) (indicated by circle) with one, two or three days' duration and identified in pixel diagram by olive red and/or red colours. Recurrent activity is characterized by recurrent red or olive red colours without begging SSC days. Quiet days activity is given by white and blue colours with the other days contributing to fluctuating activity. Each class of activity can be shown in Figure 8.

It emerges from Figure 8 with respect to the work of Ouattara (2009) that asymmetries are more due to intense solar activity during October month than during March month. In pixel diagram of the year 1999 (Figure 8a), the asymmetry results from fluctuating activity due to

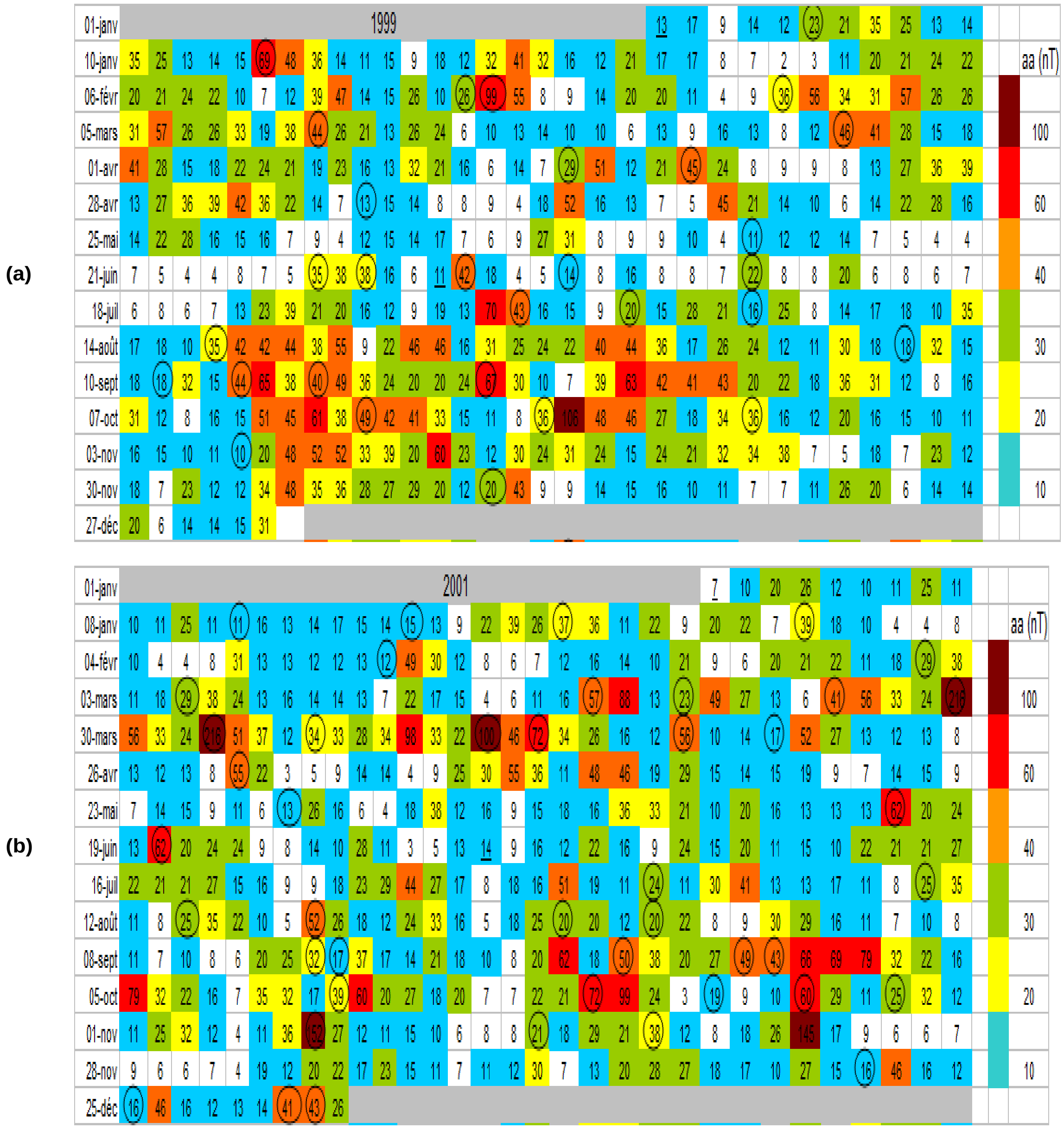

Figure 8. Pixel diagrams of years 1999 (panel a) and 2001 (panel b).

the fluctuating solar wind (Ouattara, 2009) provoked by the fluctuation of solar neutral sheet (Legrand and Simon, 1989). In pixel diagram of the year 2001 (Figure 8b), the asymmetry is due to CMEs (Ouattara, 2009). Thus, the results obtained from the analysis of pixel diagrams and from the use of Ap index are the same.

d) CODG TEC asymmetry source according to the results of Cliver et al. (2002)

Cliver et al. (2002) gives the dates of peaks of semi-annual variation of geomagnetic index aa during quiet time and disturbed period and the mechanism that likely explained such variation. The periods of the peak occurrence obtained from their work is given in the top of Tables 1 (disturbed period) and 2 (quiet period). For analysing the results of this research, the gap (shown by Δ in the table) between their peak date with respect to the mechanism and the observed peak date was determined. Observed dates are indicated in red and the possible mechanism is given by minimum value of Δ. This minimum value is highlighted in green.

Tables 1 and 2 show that the semi-annual variation of CODG TEC at Niamey during the years 1999 and 2001 is managed by Russell McPherron mechanism.

Table 1. Disturbed period (aa >20 nT).

Parameter		Spring maximum	Fall Maximum	Summer minimum	Winter minimum
Axial		7 March	9 September	7 June	8 December
Russell McPherron		7 April	11 October	7 July	6 January
Equinoctial		21.1 March	23.4 September	21.8 June	22.3 December
1999	Observed date	14.6 March	16.6 November	2.6 July	23.5 January
	Δ Axial (days)	+7.6	+68.6	+25.6	+46.5
	Δ Russell McPherron (days)	-23.4	**+36.6**	**-4.4**	**+17.5**
	Δ Equinox (days)	**- 6.5**	+ 54.2	+ 11.8	+ 33.2
2000	Observed date	06.6 April	27.5 October	12.6 June	20.5 January
	Δ Axial (days)	+30.6	+48.5	+5.6	+43.5
	Δ Russell McPherron (days)	**-0.4**	**+16.5**	-24.4	**+14.5**
	Δ Equinox (days)	+ 16.5	+ 34.1	**- 9.2**	+ 32.2
2001	Observed date	14.7 April	10.5 November	15.5 July	26.5 January
	Δ Axial (days)	+38.7	+62.5	+38.5	+49.5
	Δ Russell McPherron (days)	**+7.7**	**+30.5**	**+8.5**	**+20.5**
	Δ Equinox (days)	+ 24.6	+ 48.1	+ 23.7	+ 35.2
2002	Observed date	03.6 March	28.5 October	29.6 July	24.6 December
	Δ Axial (days)	**-3.4**	+49.5	+52.6	+16.6
	Δ Russell McPherron (days)	-34.7	**+17.5**	**+22.6**	-12.4
	Δ Equinox (days)	- 14.5	35.1	+ 37.8	**+ 02.3**
2003	Observed date	10.6 March	28.5 October	20.5 July	05.6 December
	Δ Axial (days)	**+3.6**	+49.5	+43.5	**-2.4**
	Δ Russell McPherron (days)	-27.4	**+17.5**	**+13.5**	-31.4
	Δ Equinox (days)	- 10.5	35.1	+ 28.7	- 16.7
2004	Observed date	03.6 April	23.6 October	17.6 July	06.5 December
	Δ Axial (days)	+27.6	+44.6	+40.6	**-1.5**
	Δ Russell McPherron (days)	**-3.4**	**+12.6**	**+10.6**	-30.5
	Δ Equinox (days)	+ 13.5	+ 30.2	+ 25.8	- 15.8
2005	Observed date	14.6 March	17.6 September	02.6 July	02.6 December
	Δ Axial (days)	+7.6	+8.6	+25.6	**-5.4**
	Δ Russell McPherron (days)	-23.4	-23.4	**-4.4**	-34.4
	Δ Equinox (days)	**- 6.5**	**- 5.8**	+ 10.8	- 19.7
2006	Observed date	14.7 April	10.5 November	05.5 July	23.7 January
	Δ Axial (days)	+38.7	+62.5	+28.5	+46.7
	Δ Russell McPherron (days)	**+7.7**	**+30.5**	**-1.5**	**+17.7**
	Δ Equinox (days)	+ 24.6	+ 48.1	+ 13.7	+ 32.4
2007	Observed date	25.6 March	03.6 October	14.6 June	17.6 December
	Δ Axial (days)	+18.7	+24.6	+7.6	+9.6
	Δ Russell McPherron (days)	-12.4	**-7.4**	-22.4	-19.4
	Δ Equinox (days)	**+ 4.5**	+ 10.2	**- 7.2**	**- 4.7**
2008	Observed date	23.6 April	12.6 October	12.6 July	23.6 December
	Δ Axial (days)	+47.6	+33.6	+35.6	+15.6
	Δ Russell McPherron (days)	**+16.6**	**+1.6**	**+5.6**	-13.4
	Δ Equinox (days)	+ 33.5	+ 19.2	+ 20.8	**+ 1.3**

Table 2. Quiet period (aa≤ 20 nT).

Parameter		**Spring maximum**	**Fall maximum**	**Summer minimum**	**Winter minimum**
Axial		7 March	9 September	7 June	8 December
Russell McPherron		7 April	11 October	7 July	6 January
Equinoctial		21.1 March	23.4 September	21.8 June	22.3 December
1999	Observed date	18.6 March	26.6 November	4.6 July	04.5 January
	Δ Axial (days)	+9.6	+78.6	+27.6	+27.5
	Δ Russell McPherron (days)	-19.4	**+43.4**	**-2.4**	**-1.5**
	Δ Equinox (days)	**- 2.5**	+ 64.2	+ 12.6	+ 13.2
2000	Observed date	13.5 April	29.6 October	01.5 June	13.5 January
	Δ Axial (days)	+37.5	+50.6	-5.5	+36.5
	Δ Russell McPherron (days)	**+6.5**	**+18.6**	-35.5	**+7.5**
	Δ Equinox (days)	+ 24.4	+ 36.2	**- 20.6**	+ 22.2
2001	Observed date	29.6 April	03.5 October	12.6 July	11.5 January
	Δ Axial (days)	+53.6	+24.5	+35.6	+34.5
	Δ Russell McPherron (days)	**+22.6**	**-7.5**	**+5.6**	**+5.5**
	Δ Equinox (days)	+ 39.5	+ 43.1	+ 20.8	+ 20.2
2002	Observed date	13.5 March	13.5 October	28.5 July	10.6 December
	Δ Axial (days)	**+6.5**	+34.5	+51.5	**+2.6**
	Δ Russell McPherron (days)	-24.5	**+2.5**	**+21.5**	-26.4
	Δ Equinox (days)	- 7.6	+ 20.1	+ 36.7	- 11.7
2003	Observed date	12.7 March	27.6 October	22.6 July	01.6 December
	Δ Axial (days)	+5.7	+48.6	+45.6	**-6.4**
	Δ Russell McPherron (days)	-25.3	**+16.6**	**+15.6**	-35.4
	Δ Equinox (days)	**- 8.9**	+ 34.2	+ 30.8	- 20.6
2004	Observed date	01.6 April	27.6 October	01.4 July	03.5 December
	Δ Axial (days)	+25.6	+48.6	+24.4	**-4.5**
	Δ Russell McPherron (days)	**-5.4**	**+16.6**	**-5.6**	-31.5
	Δ Equinox (days)	+ 22.7	+ 34.2	+ 09.6	- 18.8
2005	Observed date	24.7 March	23.6 September	04.6 August	04.5 December
	Δ Axial (days)	+17.7	+14.6	+58.6	-3.5
	Δ Russell McPherron (days)	-13.3	-17.4	**+28.6**	-32.5
	Δ Equinox (days)	**+ 3.6**	**+ 00.2**	+ 43.8	**- 17.8**
2006	Observed date	29.6 April	08.5 November	23.6 August	02.5 January
	Δ Axial (days)	+53.6	+65	+77.5	+25.5
	Δ Russell McPherron (days)	**+22.6**	**28.5**	**+47.6**	**-3.5**
	Δ Equinox (days)	+39.5	+ 46.1	+ 62.8	+ 11.2
2007	Observed date	01.5 April	15.6 October	08.6 August	04.5 December
	Δ Axial (days)	+25.5	+36.6	+62.6	**-3.5**
	Δ Russell McPherron (days)	**-5.5**	**+4.6**	**+32.6**	-32.5
	Δ Equinox (days)	+ 11.4	+ 22.2	+ 47.8	-17.8

Table 2. Contd.

2008	Observed date	26.6 March	28.6 October	15.6 July	12.5 December
	∆ Axial (days)	+19.6	+49.6	+38.6	+4.5
	∆ Russell McPherron (days)	-11.4	**+17.6**	**+8.6**	-24.5
	∆ Equinox (days)	**+ 5.5**	+ 35.2	+ 23.8	**- 9.8**
2009	Observed date	25.7 March	22.6 October	20.5 August	14.5 January
	∆ Axial (days)	+18.7	+43.6	+74.5	+37.5
	∆ Russell McPherron (days)	-12.3	**+11.6**	**+44.5**	**+8.5**
	∆ Equinox (days)	**+ 4.6**	+ 29.2	+ 59.7	+ 23.2

Table 3. Synthesis of mechanism occurrence.

Season	Asymmetry mechanism	Mechanism occurrence
Quiet period		
Spring	Axial	2/11
	McPherron	4/11
	Equinoctial	5/11
Fall	Axial	
	McPherron	10/11
	Equinoctial	1/11
Summer	Axial	
	McPherron	10/11
	Equinoctial	1/11
Winter	Axial	4/11
	McPherron	6/11
	Equinoctial	1/11
Disturbed period		
Spring	Axial	2/10
	McPherron	5/10
	Equinoctial	3/10
Fall	Axial	
	McPherron	9/10
	Equinoctial	1/10
Summer	Axial	
	McPherron	8/10
	Equinoctial	2/10
Winter	Axial	3/10
	McPherron	4/10
	Equinoctial	3/10

The presence of equinoctial peak asymmetry for the year 2001 cannot be explained by the change mechanism for it is the same mechanism for March/April and for September/October.

During year 1999, the asymmetry may be explained by the change of mechanism. During March/April, the mechanism is equinoctial and during September/October it is Russell McPherron.

Only the year 2006 semi-annual variation is completely explained by Russell McPherron mechanism and that during both quiet and disturbed periods.

The synthesis (Table 3) of the mechanism that occurs during the 11 years involved (quiet time) and 10 years involved (disturbed period) shows that Russell McPherron mechanism can be used to explain the CODG TEC semi-annual variation at Niamey Station.

Conclusion

Seasonal CODG TEC presents semi-annual variation with maximum TEC observed between 1000 - 1500 UTC. The peak is seen at 1400 UTC. The seasonal CODG TEC shows equinoctial peak asymmetry. March/April peak amplitude is higher than that of September/October except during 1999 and 2001. Ap values analysis and pixel diagrams investigation show that peak asymmetry is due to moderate solar wind during 1999 and similar to CMEs during 2001. This study argues that in 2001 the asymmetry cannot be explained by the change in solar activity while this situation seems to be the cause of the asymmetry observed during 1999. The overview of TEC behaviour shows that Russell McPherron mechanism manages the semi-annual variation of TEC at Niamey station.

CONFLICT OF INTERESTS

The authors have not declared any conflict of interests.

REFERENCES

Ahluwalia HS (2000). Ap time variations and interplanetary magnetic field intensity. J. Geophys. Res. 105(A12):27481-27487.
Ahluwalia HS, Xue SS, Fikani MM (1994). Geomagnetic activity index

and solar wind speed for solar cycles, in 8th International Solar-Terrestrial Physics Symposium, Sendai edited by H. Oya, G. Rostoker 1(120). Tohuko University Press Sendai.

Bohlin JD (1977). Extreme-ultraviolet observations of coronal holes. Sol. Phys. 51:377

Chakraborty SK, Hajra R (2008). Solar control of ambient ionization of the ionosphere near the crest of the equatorial anomaly in the Indian zone. Ann. Geophys. 26:47.

Chakraborty SK, Hajra R (2010). Variability of total electron content near the crest of the equatorial anomaly during moderate geomagnetic storms. J. Atmos. Sol. Terr. Phys. 72:900.

Chapman S, Bartels J (1940). Geomagnetism. Vol. 2. Oxford Univ. Press, London P 601.

Cliver EW, Kamide Y, Ling AG (2000). Mountains vs. valleys: The semiannual variation of geomagnetic activity. J. Geophys. Res. 105:2413.

Cliver EW, Kamide Y, Ling AG (2002). The semiannual variation of geomagnetic activity: phases and profiles for 130 years of aa data. J. Atmos. Sol. Terr. Phys. 64:47–53.

Crooker NU, Feynman J, Gosling JT (1977). On high correlation between long term averages of solar wind speed and geomagnetic activity. J. Geophys. Res. 82:1933-1937.

Dessler AJ, Fejer JA (1963). Interpretation of Kp index and M-region geomagnetic storms, Planet. Space Sci. 11:505-511.

Gosling JT (1976). Transient phenomena in the solar atmosphere and solar wind, in Physics of Solar Planetary Environments, edited by DJ. Williams, AGU pp. 286-303.

Green CA (1984). The semiannual variation in the magnetic activity indices Aa and Ap. Planet. Space Sci. 32:297.

Hajra R, Echer E, Tsurutani BT, Gonzalez WD (2013). Solar cycle dependence of High-Intensity Long-Duration Continuous AE Activity (HILDCAA) events, relativistic electron predictor? J. Geophys. Res. 118:5626.

Hajra R, Chakraborty SK, Tsurutani BT, DasGupta A, Echer E, Brum CGM, Gonzalez WD, Sobral JHA (2016). An empirical model of ionospheric total electron content (TEC) near the crest of the equatorial ionization anomaly (EIA). J. Space Weather Space Clim. 6:A29.

Legrand JP, Simon PA (1989). Solar cycle and geomagnetic activity: A review for geophysicists. Part I. The contributions to geomagnetic activity of shock waves and of the solar wind. Ann. Geophys. 7(6):565-578.

Mayaud PN (1968). Indices Kn, Ks et Km, 1964-1967, 156 pages, Ed. CNRS, Paris.

Mayaud PN (1971). Une mesure planétaire d'activité magnétique basée sur deux observatoires antipodaux. Ann. geophys. 27:71.

Mayaud PN (1972). The aa indices: a 100-year series characterizing the magnetic activity. J. Geophys. Res. 77(34):6870-6874.

Mayaud PN (1973). A hundred year series of geomagnetic data. 1868-1967, IAGA Bull. 33, Zurich 251p.

Murayama T (1974). Origin of the semiannual variation of geomagnetic Kp indices. J. Geophys. Res. 79:297.

Nanéma E, Ouattara F (2013). HmF2 quiet time variations at Ouagadougou and comparison with IRI-2012 and TIEGCM predictions during solar minimum and maximum. Arch. Appl. Sci. Res. 5(5):55-56.

Newkirk GA, Hundhausen J, Pizzo V (1981). Solar cycle modulation of galactic cosmic rays: Speculation on the role of coronal transients. J. Geophys. Res. 86:5387-5396.

Nolte JT, Krieger AS, Timothy AF, Gold RE, Roelof EC, Viana G, Lazarus AJ, Sullivan JD, McIntosh PS (1976). Coronal holes as sources of solar wind. Sol. Phys. 46:303-332.

Ouattara F (2009). Contribution à l'étude des composantes du champ magnétique solaire et l'ionosphère équatoriale. Thèse de Doctorat d'Etat, Faculté des Sciences et technique, université Cheikh Anta Diop, Dakar, Sénégal, 348 p.

Ouattara F, Amory Mazaudier C (2009). Solar-geomagnetic activity and Aa indices toward a standard classification. J. Atmos. Solar-Terr. Phys. 71:1736-1748.

Ouattara F, Amory-Mazaudier C, Fleury R, Lassudrie Duchesne P, Vila P, Petitdidier M (2009). West African equatorial ionospheric parameters climatology based on Ouagadougou ionosonde station data from June 1966 to February 1998. Ann. Geophys. 27:2503-2514.

Ouattara F, Ali MN, Zougmoré F (2012). A comparative study of seasonal and quiet time foF2 diurnal variation at Dakar and Ouagadougou stations during solar minimum and maximum for solar cycles 21-22. Eur. Sci. J. pp. 1-14

Rishbeth H, Muller-Wodarg ICF, Zou L, Fuller-Rowell TJ, Millward GH, Moffett RJ, Idenden DW, Aylward AD (2000). Annual and semiannual variations in the ionospheric F2-layer: II. Physical discussion. Ann. Geophys. 18:945-956.

Richardson IG, Cane HV (2002). Sources of geomagnetic activity during nearly three solar cycles (1972–2000). J. Geophys. Res. 107(A8):1187.

Richardson IG, Cliver EW, Cane HV (2000). Sources of geomagnetic activity over the solar cycle: relative importance of coronal mass ejections, high-speed streams, and slow solar wind. J. Geophys. Res. 105(A8):18200-18213.

Russell CT, McPherron RL (1973). Semiannual variation of geomagnetic activity. J. Geophys. Res. 78:92.

Simon PA, Legrand JP (1989). Solar cycle and geomagnetic activity: A review for geophysicists. Part II. The solar sources of geomagnetic activity and their links with susnspot cycle activity. Ann. Geophys. 7(6):579-594.

Snyder CW, Neugebauer M, Rao UR (1963). The solar wind velocity and its correlation with cosmic ray variations and with solar and geomagnetic activity. J. Geophys. Res. 68:6361-6370.

Svalgaard L (1977). Geomagnetic activity: dependence on solar wind parameters. In: Zirker JB (Ed.), Coronal Holes and High Speed Wind Streams. Colorado Associated University Press, Boulder P 371.

Tsurutani BT, Gonzalez WD, Gonzalez ALC, Tang F, Arballo JK, Okada M (1995). Interplanetary origin of geomagnetic activity in the declining phase of the solar cycle. J. Geophys. Res. 100:21.717-21.733.

International Journal of Physical Sciences

Related Journals Published by Academic Journals

- *African Journal of Pure and Applied Chemistry*
- *Journal of Internet and Information Systems*
- *Journal of Geology and Mining Research*
- *Journal of Oceanography and Marine Science*
- *Journal of Environmental Chemistry and Ecotoxicology*
- *Journal of Petroleum Technology and Alternative Fuels*

academicJournals